DOMAIN COMPOSITION METHOD AND ITS APPLICATIONS

by

WEI SONG

A dissertation submitted to the

Graduate School-New Brunswick

Rutgers, The State University of New Jersey

In partial fulfillment of the requirements

For the degree of

Doctor of Philosophy

Graduate Program in Mechanical and Aerospace Engineering

Written under the direction of

Professor Hae Chang Gea

And approved by

_____

_____

_____

_____

New Brunswick, New Jersey

JANUARY, 2014

ABSTRACT OF THE DISSERTATION

Domain Composition Method and its Applications

By WEI SONG

Dissertation Director:

Professor Hae Chang Gea

Topology optimization methods have been fully developed during the past two decades, and it has achieved great success in the structural design field. In topology optimization, design domain is predetermined, and it keeps unchanged in structural optimization process. However, fixed design domain is difficult to satisfy some design requirements such as domain sizing adjustment or boundaries change.

In this dissertation, Domain Composition Method (DCM) is proposed to meet this challenge. Instead of treating design domain as a whole, DCM divides domain into several subdomains at the beginning. It defines additional scaling factors and applies subdomain transformations to describe the change between different designs. Then it composites subdomains and solve it as an updated domain. Consequently, structural

analysis and sensitivity analysis can be derived. Furthermore, domain and topology of the structure are optimized simultaneously. Using DCM, regional strain energy formulation is discussed in protective structures design problem. Since the protective structures always undergo dynamic loads in practice, but the transient analysis is too expensive to apply, inertia relief analysis is employed to analyze the structure deformation. Some applications of DCM using regional strain energy formulation and inertia relief analysis are presented and discussed.

The main contributions of this dissertation are listed as follows: (1) presenting the concept of Design Composition Method (DCM), (2) applying DCM in static analysis and inertia relief analysis, (3) deriving the sensitivity of total strain energy and regional strain energy with DCM, (4) discussing the protective structures design scheme employing DCM using regional strain energy formulation and inertia relief analysis.

Acknowledgement

I would like to express my deepest appreciation to my advisor Professor Hae Chang Gea for his valuable guidance and continuous encouragement throughout my doctoral studies. His friendly advice and the high degree of motivation have been very helpful to my academic and personal aspects of my life.

I would also like to thank my committee members, Professor Liping Liu, Professor Aaron Mazzeo and Professor Kang Li, for their interest in this research and for their valuable time in reviewing my dissertation.

I wish to acknowledge my current and previous lab mates: Dr. Po-Ting Lin, Dr. Euihark Lee, Dr. Kazuko Fuchi, Dr. Xike Zhao, Huihui Qi, Bo Wang, Yanfeng Li, Dr. Zheqi Lin, Dr. Xiaobao Liu, Dr. Xiaoling Zhang, Dr. Jiantao Liu, Professor Kemin Zhou and Professor Haiqing Li. Their physical and mental supports inspire and push me forward. I would also like to give my great appreciation to my colleagues: Yang Wang, Lixin Hu and all other colleagues who may help me continue my research at some points.

I am extremely grateful to my parents and parents-in-law: Guangyin Song, Hong Ma, Jianjun Wu and Guiying Wang. Truly thank them all for their enormous encouragement and dedication during these years.

Most importantly, I want to especially devote my appreciation and love to my dear wife, Han Wu. Thank you for your sacrifice, encouragement and love. It is impossible for me to complete this research work without your accompany.

Finally, support of this work by the Department of Mechanical and Aerospace Engineering and China Scholarship Council (CSC) is deeply appreciated.

Dedication

To my dear wife

Han Wu

and my lovely daughter

Emma

Table of Contents

List of Figures

List of Tables

Chapter 1. Introduction

Structural engineers always attempt to come up with designs to enhance the efficiency of objects while designing structures and they try to improve the performance of the structures using the minimal resources. The common process generates many different designs and analyzes them to select the 'best' design but it does strongly depend on the limited knowledge and experience of the engineers. To overcome this drawback, optimization theory was introduced in structural design and then structural optimization filed was constructed.

Typically, three kinds of structural optimization problems are discussed in the literature: sizing, shape and topology optimization problems. Sizing optimization is optimized the size of each structural member for a given geometry. Shape optimization is finding out the optimal boundary of a parameterized design while keeping the topology constant with no holes created or destroyed. These two kinds of problems require a priori knowledge of the structural shape. However, for the new structural design without a priori knowledge, it might be difficult to get a concept design. Topology optimization can be used without a priori assumption of the structural shape and connectivity [1]. It is trying to find the optimal material distribution within a predefined design domain under boundary conditions.

Conventionally, the design domain in topology optimization is predefined, and it does not adjust in structural topology optimization process. Designers are required to specify the design domain in advance. In some cases, such as a package cushioning design shown in Figure 1.1, the design domain changing together takes more flexibility than only topology changing during the design process.

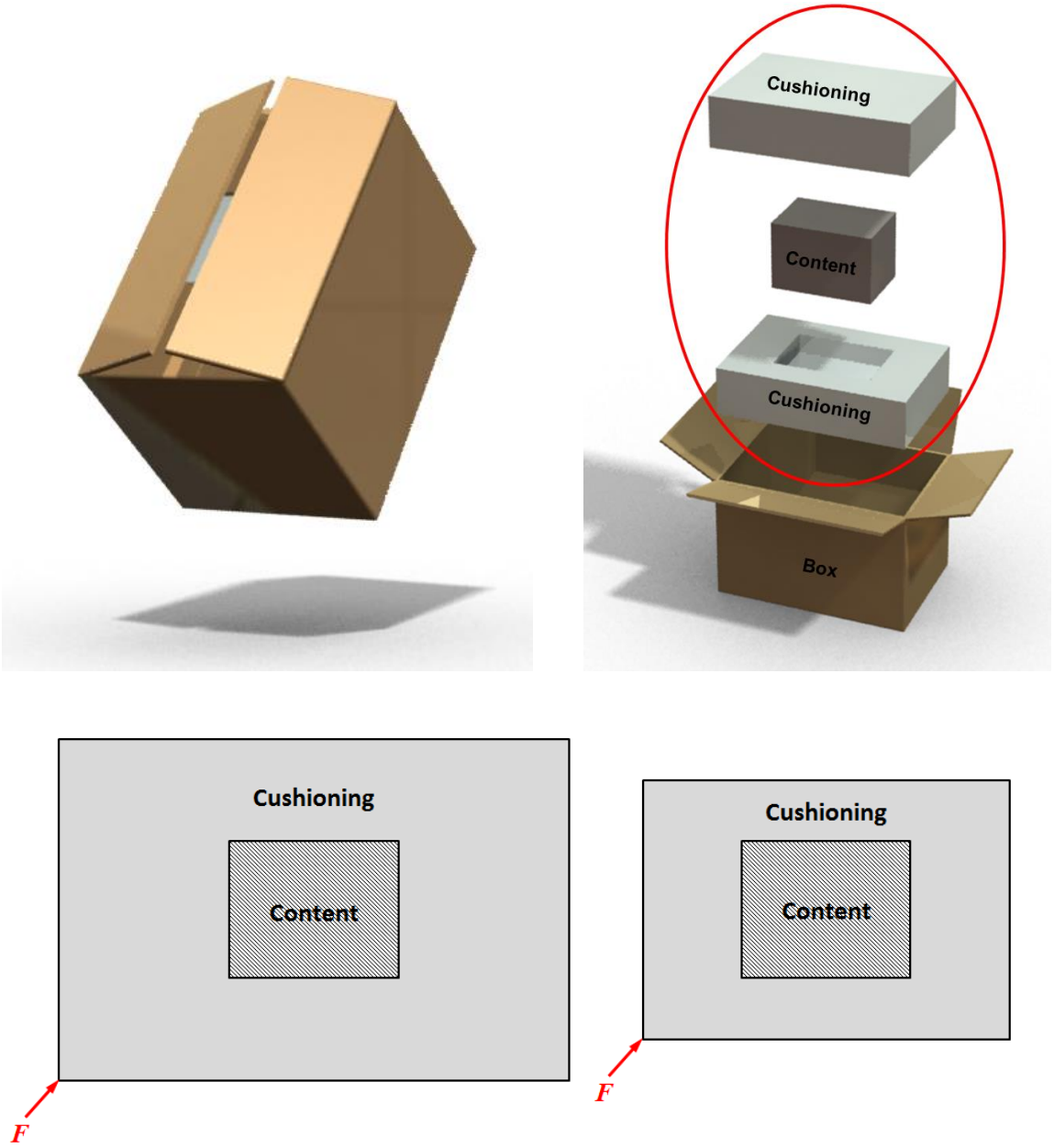

Figure 1.1. A Typical Package Cushioning Design Example: Edge Drop Test (Top Left), Package Composition (Top Right), Simplified 2D Initial Configuration (Bottom Left), Simplified 2D Shrinked Configuration (Bottom Right)

In this package cushioning design example as shown in Figure 1.1, the protection performance of the package is dependent on the proper structural design of cushioning

and only cushioning and content are considered in the simplified 2D case. Then designing a better cushioning structure with a constant material usage is a typical structural optimization problem and topology optimization can be employed here. However, the design domain is not fixed in this example, and its size might be changed during the design process. A new structural optimization method would be desired to optimize the design domain and material distribution simultaneously. Thus, a new method, Domain Composition Method (DCM), is proposed in this dissertation and it deals with the design domain and the material distribution optimization in one framework.

Furthermore, it is worth to note the goal of this cushioning design is protecting inside content but holding the structure integrity for outside cushioning. It is a multi-criteria optimization problem obviously and the conventional total strain energy formulation is not fit anymore. A new formulation based on regional strain energy formulation is suggested in this dissertation. This formulation is appropriate for protecting or strengthening part of the structure.

In practice, package undergoes drop and impact conditions in storage and transportation. It is the dynamic response of the package if the deformation analysis is required and static analysis does not apply to this situation. However, the computational cost of dynamic analysis is too expensive. An alternative cheap analysis so-called inertia relief analysis is employed in our research, and it takes into account the dynamic effects but utilizes the static analysis.

In the following section, structural optimization is to be reviewed and provide a fundamental overview on these topics.

1.1. Literature Review

The first work of structural optimization can be traced to work done by Maxwell [2] who proved that a fully stressed pin jointed truss with a given set of forces applied at specified locations, the volume difference between tension and compression members is a constant in 1869. Levy [3] and Cilley [4] studied the fully-stressed design of indeterminate pin joint frameworks in 1888 and 1900 respectively. Michell [5] proposed a theory for minimum weight structures on limits of economy of material based on the extension of Maxwell's results in 1904. This work established the theoretical basis for the structural optimization. Wasiutynsky published possible the first review of the optimum of strength design in 1939. This review, summarizing the works from Galileo to 1930, "is based on source materials and includes numerous quotations of the original texts and proofs" [6].

During the 1950s and 1960s, extensive research was developed in the minimum weight design, especially in aircraft structure components design because of the aircraft structure requirement in post-war [6]. Shanley (1952) exposed the principle of simultaneous failure modes to the solutions of problems for structural design in his book [7]. Similarly, Johnson (1961) presented the method of optimum design primarily with mechanical elements [8].

During the late 1960s and early 1970s, a structural optimization method based on Optimality Criteria (OC) was developed for the purpose of large-scale optimization [9]. It can be traced back to the work of Wasiutynski [10] in 1960. The theoretical foundation of OC was established by Prager & Taylor (1968) [11], Taylor (1969) [12] and Masur (1970) [13]. They presented the continuum problems obtain differential equations as the

optimality criteria and the solutions which provide the optimum shape of the structures. Bendsøe and Sigmund provided a comprehensive bibliographical note for Optimality Criteria (OC) method [14]. However, the OC method is not a general method since the optimality conditions are different and have to be derived on different problems, and this limits the range of its application.

The development of Mathematical Programming (MP) techniques during the late 1940s and the early 1950s and the development of the Finite Element Method (FEM) with computer technologies from 1960s made it possible to extend and simplify the structural optimization problem as a powerful tool [15]. The structural optimization problems were treated as finding the mathematical extremization of an objective function in multidimensional design variables space. The extremum was obtained by linear or nonlinear MP. The FEM can analyze more complicated problem in different physics and it can provide the function evaluation for MP method. The most important information in MP method is function value and sensitivity. It is impossible to implement structural optimization without the sensitivity analysis. Generally, design sensitivity is an indicator for measuring how well a small perturbation of design variables will affect the system response or the objective function in the optimization. Sensitivity analysis can be referred in the books written by Haug, Choi & Komkov (1986) [16] and Choi & Kim (2005) [17, 18] or the review paper written by Haftka and Adelman (1989) [19].

With the great development of computer technology after 1970s, structural optimization started a new stage. Before that time, the design goal may be to find the optimal plate thickness or the optimal truss cross section. It was so-called sizing

optimization. The main feature of the sizing optimization is the design domain and the state variable is known a priori and is fixed in the design process [14].

The developed new structural optimization method was used to design the shape of the hole or the body. It was named as shape optimization. The goal of the shape optimization is to find the optimum shape of the domain. Zienkiewich and Campbell [20] described the shape optimization based on FEM by changing the coordinates of boundary nodes in 1973. Bhavikatti and Ramakrishnan [21] represented the boundary shape in shape optimization based FEM by setting the coefficients of the polynomials in 1980. The early review of shape optimization written by Vanderplaates in 1980 and he dealt with the continuous shape parameters [22]. Some survey papers and books about shape optimization are presented by Ding (1986) [23], Haftka & Gandhi (1986) [24], Zienkiewicz & Zhu (1986) [22], Hsu (1994) [25] and Kawohl et al. (1998) [26]. The shape optimization method provides a powerful tool to engineers. However, the optimal designs are based on a predefined topology although the boundaries can be changed between the design iterations, i.e. shape optimization will not change the topology of the structure, and the optimal design has the same topology as the initial design. Also, the sensitivity is difficult to calculate because the finite element mesh is design dependent [27].

To avoid disadvantages of shape optimization, topology optimization was proposed. It transformed the optimum lay-out problem into the optimum material distribution problem. Topology optimization is to find the optimal material distribution in a predefined design domain and the only known quantities in the problem are the applied loads, the possible support conditions, and the volume of the structure to be constructed

and possibly some additional design restrictions such as the location and size of prescribed holes or solid area [14]. Topology optimization needs no additional priori knowledge of engineers, so it is a very helpful design automation tool. The basic concept of finding material distribution instead of finding lay-out was discussed briefly by Cea et al. (1973) [28] and Tartar (1979) [29].

The first implementation of the material distribution was first presented by Bendsøe & Kikuchi in 1988 [30]. Their work was based on the homogenization method which the design domain is assumed to be filled with nonhomogeneous material microstructure which is characterized by multiple variables. The equivalent homogenized material constant is calculated by using the homogenization method. This concept transforms an optimal topology design problem into an optimal material distribution problem [31]. The distribution materials with microstructures in a design domain also was discussed by Cheng & Olhoff (1981) [32], Lurie et al. (1982) [33] and Kohn & Strang (1986) [34-36]. Further early developments of the homogenization can be found in Suzuki & Kikuchi (1991) [37] and Thomsen (1991) [38]. An excellent review about homogenization and its application in topology optimization was presented by Hassani & Hinton [39-41] in 1998.

Another more common used implementation of topology optimization method is the density function interpolation method which was proposed by Bendsøe in 1989 [42] and Rozvany & Zhou in 1991 [43]. This method applied the continuous variables to replace the integer variables in the original material distribution problem. This method was then utilized by Mlejnek (1992) [44], Yang (1994) [45] and other researchers because it is efficiency, usability and easy to use. One popular and efficient selection

model is so-called Solid Isotropic Material with Penalization (SIMP) model [14]. In our research, SIMP model is used and it is discussed in Section 1.2. Other interpolation schemes with isotropic material and its discussion can refer papers and book of Bendsøe & Sigmund [14, 46] and Stolpe & Svanberg [47]. A comprehensive description and explanation of SIMP model can be found in the book of Bendsøe and Sigmund [14].

From the previous literature survey of the topology optimization, the design domain is predefined or fixed, and only a few researchers studied the topology optimization with the similar boundary change problem. Chen et al. [48] presented a shape optimization method which provided explicit parametric control of geometry and topology within a large space of free-form shapes and combined free-form and parametric shape optimization approaches. This method can deal with the boundary change problem, but the design domain itself is fixed as the initial selection. Zhu et al. [49, 50] applied the so-called coupled shape and topology optimization technique to study the layout design of the components and their supporting structures in a finite packing space. The material configuration of the supporting structures and components are optimized simultaneously based on topology optimization method. The design domain of the supporting structures is fixed, and components are meshed individually and embedded with the supporting structures meshes. This method coupled shape and topology optimization together. However, the sensitivities of the total strain energy respect to the shape parameters of the components are calculated by finite difference method which requires more analysis and smaller step size in iteration. It increases the computational cost consequently.

In this dissertation, the design domain is not fixed and it changes during the design process. The design domain and the material distribution are optimized simultaneously. The design domain is divided into a series of subdomains and material is not only distributed between elements but also between subdomains. Each subdomain change is described by different parameters and the parameters have to be compatible with each other in order to keep the compatibility of the geometry. Complete discussion is proposed in Chapter 2.

In general, most topology optimization objective formulations consider total strain energy of the whole design domain. It gives the optimal design for the largest rigidity in the whole design domain. However, in some cases, only a portion of the design domain needs to be considered as an objective. For example, it is required to design a protection structure to protect a specified object, such as designing a structure to protect the battery in electric vehicle impact or designing a container to protect content. Gea [51] proposed the concept of regional strain energy formulation and applied it in energy absorption design. In this dissertation, this concept is applied to Domain Composition Method (DCM) and extended the application of the method in protective structure design. New formulation and detailed discussion are presented in Chapter 3.

To implement the topology optimization, Finite Element Analysis (FEA) and sensitivity analysis are two essential bases. Currently, most of the topology optimization problems are focused on solving for the static problem. In reality, many structure responses are dynamical. However, computational cost of dynamic analysis is much higher than static analysis. Furthermore, the sensitivity is required by mathematical programming methods but is difficult to calculate in dynamic analysis, and it always

calculates in each time step [52]. In order to fill this gap, inertia relief analysis can be applied in domain compositing optimization problem. It takes into account the dynamic effects but utilizes the static analysis, thus saving a substantial amount of computation time and cost [53].

Inertia relief was widely used in many industries such as automotive, aerospace, flight and airship. Agrawal et al. [53] used inertia relief to analyze a hood structure under slam/drop type loading which was due to the complexity of the impact phenomenon. Mahishi [54] carried out inertia relief as the measured road loads were in self equilibrium to design the lower control arm in a suspension system. Sleight and Muheim [55] performed inertia relief analysis with geometric nonlinearity on two general square solar sail design to identify parameters of interest. Bessert and Frederich [56] employed ABAQUS inertia relief analysis and performed the nonlinear airship disturbed structure model in order to yield the respective aero-elastic derivatives. Liao and Pasternak[57] presented design and analysis cycle of buoyant air vehicle using inertia relief calculation.

On the other hand, researchers studied various inertia relief key issues and applied it to structural optimization, especially in topology optimization. Anvari and Beigi [58] compared inertia relief analysis and transient dynamics analysis in vehicle structure stress analysis to show its using condition and accuracy. Liao [59] described the principle of inertia relief analysis and discussed inertia relief capability in main current commercial finite element packages. Pagaldipti and Shyy [60] revealed inertia relief influence in structural design optimization procedure. Quinn [61] studied full automobile topology design optimization problem to maximize structural stiffness subject to multiple static load cases and compared the results of inertial relief analysis with conventional static

analysis. However, a systematical discussion of formulation and sensitivity derivations with inertia relief has rarely been found. After a concise discussion of basic equations and solving techniques of inertia relief, Domain Composition Method (DCM) is used in inertia relief analysis and applied into structural optimization problem. Complete formulation and discussion are proposed in Chapter 4.

1.2. Background of Topology Optimization

In this dissertation, Domain Composition Method (DCM) is optimized design domain and material distribution simultaneously and it can be treated as an extension of the topology optimization. It's worth to discuss some background of topology optimization for the completeness of the dissertation.

Topology optimization for continuum structures is finding the optimal distributions of the available material in a predetermined design domain [62]. Typically, the maximal stiffness in structures, i.e. the minimal strain energy or the minimal mean compliance is commonly considered as an objective, and the prescribed (constant) material volume is the constraint. The discretized topology optimization problem is stated as

$$\begin{aligned} &\underset{\boldsymbol{\gamma}}{Min}:\ U_T = \frac{1}{2}\mathbf{u}^T\mathbf{K}\mathbf{u} \\ &s.t.:\quad \mathbf{K}\mathbf{u} = \mathbf{F} \\ &\qquad V(\boldsymbol{\gamma}) \le \overline{V} \\ &\qquad \gamma_i = \gamma_{\min} \text{ or } 1,\quad i = 1,\cdots,N \end{aligned} \tag{1.1}$$

where U_T is the total strain energy of the structure. Displacement and external force vector are denoted $\mathbf{u}$ and $\mathbf{F}$, respectively. V_0 is the total volume of the design domain.

$\bar{V}$ is the constant material volume which means the maximal material usage to build the structure. Design variable γ_i indicates the material pseudo-density in the i^{th} element in finite element model. It takes 0 or 1 to indicate non-existence or existence of the given material within each element. The material pseudo-density value 0 is usually replaced by $\gamma_{\min}$, a very small positive number, to avoid the singularity in the finite element analysis.

Above discrete optimization problem is difficult to be solved by gradient-based optimization algorithms, because design variables are not continuous. In order to utilize the fully developed continuous optimization methods, some material interpolation models had been proposed. One of the most commonly used material models is so-called "power-law approach" or Solid Isotropic Material with Penalty (SIMP) model [30, 42, 43, 46, 63]. SIMP model employs the following power-law relation to describe the stiffness and the mass of a material with the pseudo-density γ_i

$$E_i = \gamma_i^p E_0$$

$$\rho_i = \gamma_i \rho_0$$

where γ_i is a continuous pseudo-density $0 < \gamma_{\min} \le \gamma_i \le 1$. p represents a penalty coefficient to material, which is set to a value greater than 1 to provide a penalty on stiffness of the material. In general, it always sets $p = 3$ [63] and it also happens in our research. E_0 and ρ_0 represent Young's modulus and density of a given material.

The effect of different penalty values p to the relative stiffness (E/E_0) is illustrated in Figure 1.2. As shown in this figure, the curve has a tendency towards a step function when the penalty power p increases. Therefore, topology optimization method

can be more efficient to converge material density (γ_i) as a void ($\gamma_i = \gamma_{\min}$) or solid ($\gamma_i = 1$) in SIMP model. Hence, the result of topology optimization will tend to an optimal design with mostly solid and void phase [42].

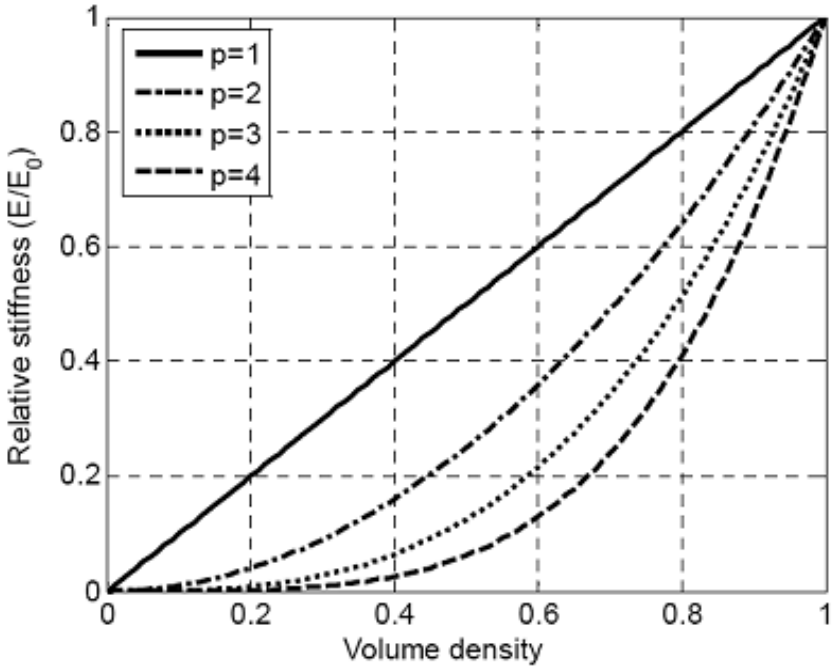

Figure 1.2. Penalization of the Intermediate Pseudo-density in SIMP Model [42]

Applying SIMP model in original topology optimization problem (1.1), the discretized optimization problem is relaxed to a continuous optimization problem as

$$\begin{aligned} &\underset{\boldsymbol{\gamma}}{Min}: \; U_T = \frac{1}{2}\mathbf{u}^T\mathbf{K}\mathbf{u} \\ &s.t.: \quad \mathbf{K}\mathbf{u} = \mathbf{F} \\ &\qquad V(\boldsymbol{\gamma}) \le \overline{V} \\ &\qquad 0 < \gamma_{\min} \le \gamma_i \le 1, \;\; i = 1, \cdots, N \end{aligned} \tag{1.2}$$

In this study, this relaxation of material distribution design variables is the same as appearing in formulation (1.2).

1.3. Research Contribution

Domain Composition Method (DCM) for structural optimization is presented and developed in this dissertation. Several achievements are summarized as follows:

- ***The concept of DCM***

The design domain changing problems are difficult to handle in structural optimization because traditional domain parameterization has to apply finite difference method to calculate the sensitivity for the optimization algorithm rather than accurate derivation. In this dissertation, design domain is divided into subdomains, and the transformation relations are constructed by defining parameters in subdomains. These subdomain transformation relations are combined into analysis and sensitivity calculation procedure.

- ***Static analysis and inertia relief analysis using DCM***

In this study, DCM is applied in static analysis and inertia relief analysis. Element stiffness matrices and element mass matrices are derived by applying subdomain transformations between the current design domain and the initial design domain. Global stiffness matrix and global mass matrix of the current design domain can be expressed by parameters which are defined in corresponding subdomains. Static analysis and inertia analysis using DCM are described in Chapter 2 and Chapter 4 respectively.

- ***Sensitivity analysis with DCM***

Accurate sensitivity analyses are derived for static analysis and inertia relief analysis using DCM. Two types of objective functions are considered, total strain energy

formulation and regional strain energy formulation. In Chapter 2, the sensitivity of total strain energy with static analysis is derived. In Chapter 3, the sensitivity of regional strain energy with static analysis is considered. In Chapter 4, the sensitivity of regional strain energy with inertia relief analysis is obtained. All sensitivities are derived with respect to two kinds of design variables: conventional material distribution variables and new defined parameters in subdomains.

- ***Protective structure design using DCM***

Two physics of the protective structure design problems are proposed in Chapter 3 and Chapter 4: static analysis and inertia relief analysis. The static analysis covers the structure static response meanwhile the inertia relief analysis deals the structure dynamical response. The proposed regional strain energy formulation is good for design protecting or strengthening a part of structure. It is straightforward to apply to protective structure design such as the above cushioning design example.

1.4. Outline of the Dissertation

This dissertation consists of five chapters discussing Domain Composition Method (DCM) and its applications. Furthermore, the protective structure optimization is mainly considered such as the package cushioning design. All the details are introduced and discussed in the rest of the dissertation.

The remainder of this dissertation is organized as follows:

In Chapter 2, DCM is studied. The design domain in topology optimization is discussed. If the wholly or partial of the domain is changed, the optimization may give a better solution than the fixed design domain situation. The sensitivity of the design domain changing is difficult to calculate using the conventional parameterization. To

solve this problem, DCM is presented and illustrated in the static analysis. The total strain energy formulation with static analysis using DCM is proposed. The sensitivities of the total strain energy formulation with respect to the material distribution variable and subdomain parameters are derived. Two numerical examples are presented in this chapter: one is a package cushioning design and another one is a cantilever beam with a movable hole design.

In Chapter 3, DCM using the regional strain energy formulation is presented. Considering the protective structure design, the protected region is the design focus and is naturally to minimize the strain energy in this region but the structure integrity is required at the same time. To tradeoff this multi-criteria optimization problem, the multiplication of total strain energy and regional strain energy is employed, and then the sensitivities with respect to two kinds of design variables are obtained. Two examples are discussed: one is the same example discussed in Chapter 2, but uses the regional strain energy formulation; another one is an extension of this formulation to support structure design application.

In Chapter 4, inertia relief analysis is employed to analyze the dynamical response in the protective design. The equations and solving technique of inertia relief analysis are presented. The structural optimization problem is formulated using DCM with inertia relief. DCM is combined with the inertia relief analysis and the sensitivities for two types of design variables are derived. The cushioning design example is offered.

Finally, the main conclusions of this research are briefly summarized and the further extensions of the current work are proposed in Chapter 5.

Chapter 2. Domain Composition Method (DCM)

Structural optimization, in particular topology optimization, has been introduced in the previous chapter; this chapter starts from the discussion of design domain in topology optimization. Design domain are typically considered predefined in traditional topology optimization, and some designers' need to find the most effective way to set up design domains is not addressed. This leads to an introduction of Domain Composition Method (DCM) which divides design domain into several subdomains to describe the size of domain change but solves problem after subdomains composition. In this chapter, DCM is described and combined into static analysis. A new structural optimization based on DCM is then introduced, and its sensitivity is derived.

2.1. Design Domain in Topology Optimization

In structural optimization, topology optimization of solid structures is to determine the number, location and shape of holes and the connectivity of domain [14]. Typical topology optimization problems are formulated as problems to find the optimal material distribution in fixed design domains. Generally, selection of the design domain is based on a priori knowledge including designer's preference, the objective function, relevant physics, geometric constraints, boundary conditions, external loads and manufacturing concerns. For example, Figure 2.1 depicts a typical selection of a design domain for the given boundary condition and external force. In this case, the design domain is fixed.

Figure 2.1. A Typical Selection of Design Domain in Topology Optimization

However, if the design domain is flexible to choose, such as the cushioning design example discussed in Chapter 1, which is a static version of this problem shown in Figure 2.2, the cushioning design are flexible to select in some ranges and the optimization may give a better solution by combining the material distribution and the design domain changing. In structural optimization, a parametric shape is described by a set of geometric parameters called dimensions [48]. Parameterization of the dimensions is needed in order to implement this idea.

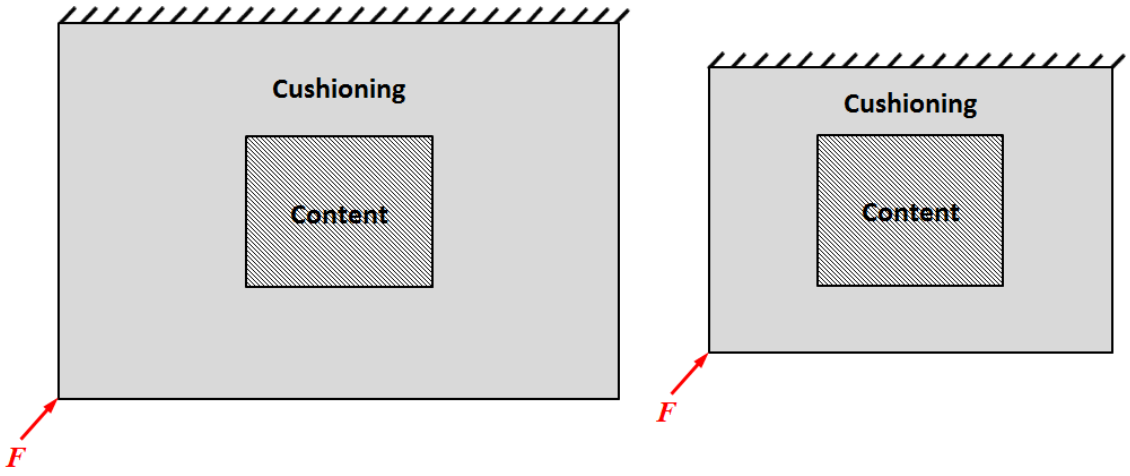

Figure 2.2. Flexibility of Selection Design Domain

A straightforward parameterization for this example is shown in Figure 2.3. In this circumstance, two dimensions parameterize the thicknesses of cushioning if the cushioning is symmetric in both directions. However, this parameterization is difficult to combine with the existing topology optimization procedure mainly because the sensitivity of parameters such as lengths and heights cannot be derived analytically. The finite difference method can be applied, but it has some severe drawbacks. If n parameters are defined in the design problem, $n+1$ analysis will be required to calculate the sensitivity information in each iteration of the structural optimization problem. Furthermore, in order to keep the accuracy of sensitivity results, the change between iterative steps need be kept small enough. The step size has to be as small as 10^{-5} times the difference between the parameter's upper and lower bounds, i.e. $\Delta = 10^{-5}(ub - lb)$. Consequently, the convergence of the optimization problem becomes unacceptably slow and it makes the finite difference method undesirable.

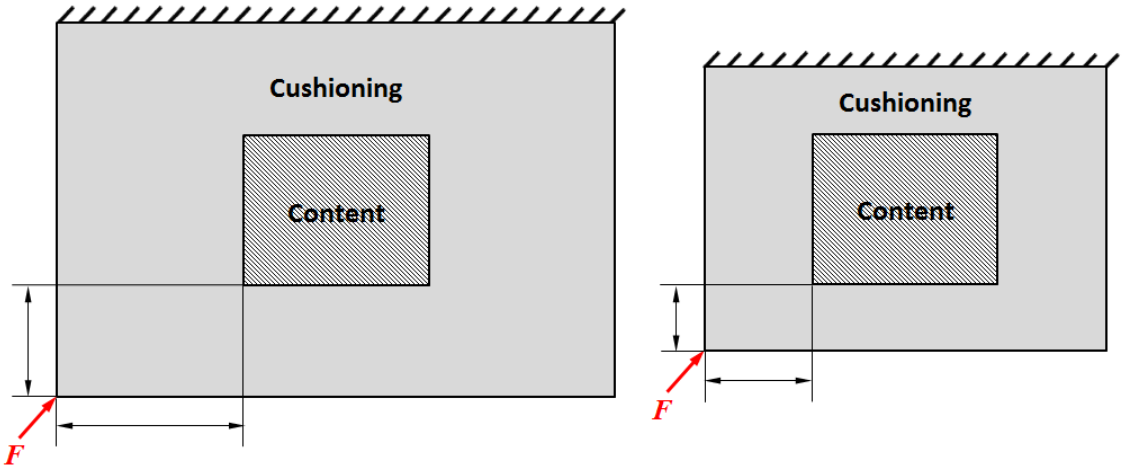

Figure 2.3. Traditional Parametrization for Two Different Configurations

In order to overcome the difficulties discussed above, a new parameterization method is presented in the following section.

2.2. Domain Composition Method (DCM)

In previous section, the same topology optimization problem but the different design domains was discussed. If the flexible design domain can be found the optimal configuration, the designer is provided a better design than traditional topology optimization. To touch this goal, the parameterization of the design domain is needed. The traditional parameterization method applies finite difference method to calculate the sensitivity for the optimization algorithm rather than accurate derivation. It has downside, such as it requires more analyses and too small step size in iterations. To overcome the existing drawbacks, a new parameterization of the design domain is proposed.

2.2.1. Domain Division

To illustrate the proposed parameterization method, example shown in Figure 2.3 will be considered. In order to change the size of cushioning, the entire domain is divided into a set of subdomains, and then the dimensions of subdomains are changed correspondingly, while satisfying the geometric compatibility as shown in Figure 2.4. The cushioning changing is implemented by changing dimensions of the different subdomains. Dimensions of all the subdomains except the subdomain of the content need be changed. In order to discuss the parameterization of the dimensions, an arbitrary subdomain is selected to study.

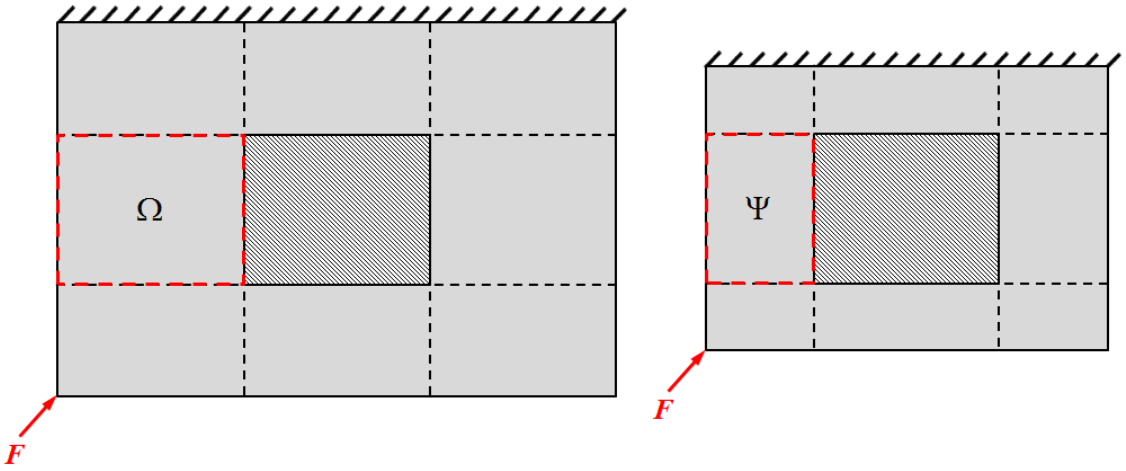

Figure 2.4. Domain Division of Design Domains: Initial Design Domain (Left) and Current Design Domain (Right)

2.2.2. Subdomain Transformation

To illustrate subdomains change in different designs, the finite element mesh is considered. The selected subdomain in initial design is denoted as Ω, and the corresponding subdomain in current design is denoted as Ψ and shown in local coordinate systems in Figure 2.5. These two subdomains have the same meshing pattern. If the dimensions of the selected subdomain of initial design are known, then the selected subdomain of current design can be parameterized by defining two scaling factors λ_x and λ_y.

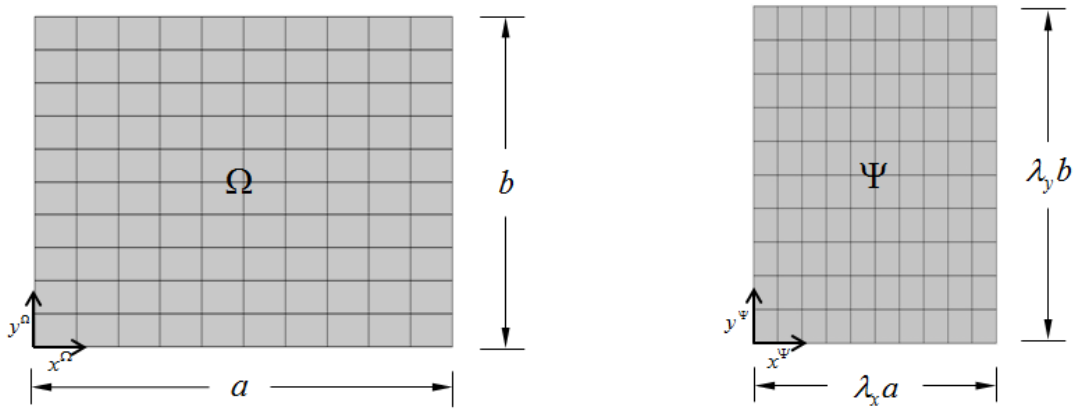

Figure 2.5. Selected Subdomain Dimensions and Defining Scaling Factors

It can be assumed that the coordinates of the subdomains Ψ and Ω have the following transformation relation

$$\begin{Bmatrix} x^{\Psi} \\ y^{\Psi} \end{Bmatrix} = \mathbf{S} \begin{Bmatrix} x^{\Omega} \\ y^{\Omega} \end{Bmatrix} \tag{2.1}$$

where S is the transformation matrix

$$\mathbf{S} = \begin{bmatrix} \lambda_x & 0 \\ 0 & \lambda_y \end{bmatrix}$$

This transformation relation provides a convenient way to parameterize dimension changes of the subdomains among different designs. This transformation was originally applied to the microstructure base cells mapping and calculation of the homogenized material properties by Liu et al. [64]. In this dissertation, this subdomain transformation is used in the structure change and it is applied in essential analysis and sensitivity derivations.

2.2.3. Static Analysis using Domain Composition Method (DCM)

In this section, linear elastic static analysis based on a finite element method is used to illustrate DCM. The same example of the package cushioning design is considered here.

As shown in Figure 2.6, six scaling factors are defined in order to describe the dimensions of the subdomains. The dimension of the inside content does not change in design process, so λ_2 and λ_5 are set equal to constant value 1. The design domain is symmetric in both directions, which means that two pairs λ_1 and λ_3 as well as λ_4 and λ_6 are equal to each other. Therefore, only two variables are necessary to parameterize the thicknesses of the cushioning, and it is consistent with traditional parameterization shown in Figure 2.3.

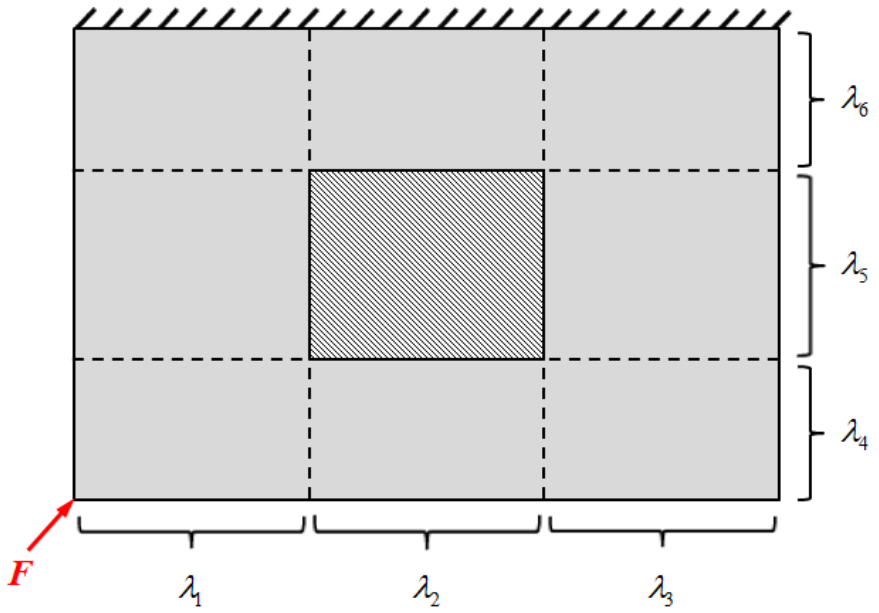

Figure 2.6. Example of Initial Design Domain Division and Scaling Factors in Subdomains

To apply the domain composition to static analysis, we denote the current design as C and the initial design as I, and the static analysis equation of the current design with an external load vector $\mathbf{F}$ is stated as

$$\mathbf{K}^C\mathbf{u}^C = \mathbf{F} \tag{2.2}$$

where

$$\mathbf{K}^C = \mathop{\mathbf{A}}_{e=1}^{N} \mathbf{k}_e^C \tag{2.3}$$

The global stiffness matrix $\mathbf{K}^C$ is assembled from element stiffness matrices of the current design C. If all element stiffness matrices are known, the global stiffness matrix can be assembled and the displacement field can be computed by solving Eq. (2.2).

Since different subdomains have different scaling factors, one element of the arbitrary subdomain Ψ in current design C is considered. The subdomain Ψ is transformed from the corresponding subdomain Ω in initial design, and scaling factors are assumed (λ_x, λ_y) as shown in Figure 2.5.

From the isoparametric formulation of Q4 element (Quadrilateral Four Nodes Element) in finite element theory, the element stiffness matrix $\mathbf{k}_e^{\Psi}$ of element e in the current design can be calculated as [65]

$$\begin{aligned} \mathbf{k}_e^{\Psi} &= \int_{V_e} \mathbf{B}^{\Psi T}\mathbf{E}\mathbf{B}^{\Psi} dV \\ &= \int_{-1}^{1}\int_{-1}^{1} \mathbf{B}^{\Psi T}\mathbf{E}\mathbf{B}^{\Psi} J^{\Psi} d\xi d\eta \end{aligned} \tag{2.4}$$

where ξ and η are isoparametric coordinates: they are not related to the nodal coordinates of the geometry model. $\mathbf{E}$ is a symmetric matrix of material stiffness. For an

isotropic material, it is equal to the following equation for a given elastic modulus E and Poisson's ratio ν are given:

$$\mathbf{E} = \frac{E}{1-\nu^2}\begin{bmatrix} 1 & \nu & 0 \\ \nu & 1 & 0 \\ 0 & 0 & \frac{1-\nu}{2} \end{bmatrix} \tag{2.5}$$

Scalar J^{Ψ} is the determinant of the Jacobian matrix $\mathbf{J}^{\Psi}$ which can be calculated as

$$\mathbf{J}^{\Psi} = \mathbf{D}_{\mathbf{N}}\begin{bmatrix} x_1^{\Psi} & y_1^{\Psi} \\ x_2^{\Psi} & y_2^{\Psi} \\ x_3^{\Psi} & y_3^{\Psi} \\ x_4^{\Psi} & y_4^{\Psi} \end{bmatrix} \tag{2.6}$$

For bilinear element, it has

$$\mathbf{D}_{\mathbf{N}} = \frac{1}{4}\begin{bmatrix} -(1-\eta) & (1-\eta) & (1+\eta) & -(1+\eta) \\ -(1-\xi) & (1-\xi) & (1+\xi) & -(1+\xi) \end{bmatrix} \tag{2.7}$$

The nodal coordinates of subdomain Ψ of the current design can be transformed from the corresponding nodal coordinates of subdomain Ω in the initial design. Applying the transformation relation defined in Eq. (2.1), Eq. (2.6) can be rewritten as

$$\mathbf{J}^{\Psi} = \mathbf{D}_{\mathbf{N}}\begin{bmatrix} x_1^{\Omega} & y_1^{\Omega} \\ x_2^{\Omega} & y_2^{\Omega} \\ x_3^{\Omega} & y_3^{\Omega} \\ x_4^{\Omega} & y_4^{\Omega} \end{bmatrix}\begin{bmatrix} \lambda_x & 0 \\ 0 & \lambda_y \end{bmatrix} = \mathbf{D}_{\mathbf{N}}\begin{bmatrix} x_1^{\Omega} & y_1^{\Omega} \\ x_2^{\Omega} & y_2^{\Omega} \\ x_3^{\Omega} & y_3^{\Omega} \\ x_4^{\Omega} & y_4^{\Omega} \end{bmatrix}\mathbf{S} = \mathbf{J}^{\Omega}\mathbf{S} \tag{2.8}$$

Thus, the determinant of the Jacobian matrix can be computed as

$$J^{\Psi} = \det(\mathbf{J}^{\Omega}\mathbf{S}) = \det(\mathbf{S})\det(\mathbf{J}^{\Omega}) = \lambda_x \lambda_y J^{\Omega} \tag{2.9}$$

In Eq. (2.4), the strain-displacement matrix $\mathbf{B}^{\Psi}$ can be expanded as

$$\mathbf{B}^{\Psi} = \mathbf{A}\mathbf{T}^{\Psi}\mathbf{N}_{\mathbf{D}} \tag{2.10}$$

where $\mathbf{A} = \begin{bmatrix} 1 & 0 & 0 & 0 \\ 0 & 0 & 0 & 1 \\ 0 & 1 & 1 & 0 \end{bmatrix}$ is a constant matrix and $\mathbf{T}^{\Psi} = \begin{bmatrix} \mathbf{\Gamma}^{\Psi} & \mathbf{0} \\ \mathbf{0} & \mathbf{\Gamma}^{\Psi} \end{bmatrix}$ is related to the nodal coordinates in subdomain Ψ. Matrix $\mathbf{N}_{\mathbf{D}}$ is the derivatives with respect to isoparametric coordinates η and ξ

$$\mathbf{N}_{\mathbf{D}} = \begin{bmatrix} N_{1,\xi} & 0 & N_{2,\xi} & 0 & N_{3,\xi} & 0 & N_{4,\xi} & 0 \\ N_{1,\eta} & 0 & N_{2,\eta} & 0 & N_{3,\eta} & 0 & N_{4,\eta} & 0 \\ 0 & N_{1,\xi} & 0 & N_{2,\xi} & 0 & N_{3,\xi} & 0 & N_{4,\xi} \\ 0 & N_{1,\eta} & 0 & N_{2,\eta} & 0 & N_{3,\eta} & 0 & N_{4,\eta} \end{bmatrix}.$$

Matrix $\mathbf{\Gamma}^{\Psi}$ stands the inverse of the Jacobian matrix

$$\mathbf{\Gamma}^{\Psi} = (\mathbf{J}^{\Psi})^{-1} = (\mathbf{J}^{\Omega}\mathbf{S})^{-1} = \mathbf{S}^{-1}(\mathbf{J}^{\Omega})^{-1} = \mathbf{S}^{-1}\mathbf{\Gamma}^{\Omega} \tag{2.11}$$

Substituting Eq. (2.11) into Eq. (2.10), it gives

$$\mathbf{B}^{\Psi} = \mathbf{A}\begin{bmatrix} \mathbf{S}^{-1} & \mathbf{0} \\ \mathbf{0} & \mathbf{S}^{-1} \end{bmatrix}\mathbf{T}^{\Psi}\mathbf{N}_{\mathbf{D}} \tag{2.12}$$

where $\mathbf{T}^{\Omega} = \begin{bmatrix} \mathbf{\Gamma}^{\Omega} & \mathbf{0} \\ \mathbf{0} & \mathbf{\Gamma}^{\Omega} \end{bmatrix}$ is similar to $\mathbf{T}^{\Psi}$.

Defining a new matrix $\mathbf{A}'$ as

$$\mathbf{A}' \equiv \sqrt{\lambda_x \lambda_y}\,\mathbf{A}\begin{bmatrix} \mathbf{S}^{-1} & \mathbf{0} \\ \mathbf{0} & \mathbf{S}^{-1} \end{bmatrix} = \begin{bmatrix} \sqrt{\lambda_y/\lambda_x} & 0 & 0 & 0 \\ 0 & 0 & 0 & \sqrt{\lambda_x/\lambda_y} \\ 0 & \sqrt{\lambda_x/\lambda_y} & \sqrt{\lambda_y/\lambda_x} & 0 \end{bmatrix} \tag{2.13}$$

which is only related to the scaling factors λ_x and λ_y of subdomain Ψ in current design.

Plugging Eq. (2.12) and (2.9) into Eq. (2.4), the element stiffness matrix $\mathbf{k}_e^{\Psi}$ of subdomain Ψ in the current design domain can be expressed merely in terms of the coordinates of the subdomain Ω in the initial design domain

$$\mathbf{k}_e^{\Psi} = \int_{-1}^{1}\int_{-1}^{1} \mathbf{N_D}^T \mathbf{T}^{\Omega T} \mathbf{A}'^T \mathbf{E} \mathbf{A}' \mathbf{T}^{\Omega} \mathbf{N_D} J^{\Omega} d\xi d\eta \tag{2.14}$$

The corresponding element stiffness matrix of subdomain Ω in the initial design domain is

$$\mathbf{k}_e^{\Omega} = \int_{-1}^{1}\int_{-1}^{1} \mathbf{N_D}^T \mathbf{T}^{\Omega T} \mathbf{A}^T \mathbf{E} \mathbf{A} \mathbf{T}^{\Omega} \mathbf{N_D} J^{\Omega} d\xi d\eta \tag{2.15}$$

Comparing Eq. (2.14) with (2.15), the difference is only matrices $\mathbf{A}'$ and $\mathbf{A}$. Therefore, if the constant matrix $\mathbf{A}$ is substituted by matrix $\mathbf{A}'$ which only depends on scaling factors λ_x and λ_y, the element stiffness matrix $\mathbf{k}_e^{\Psi}$ of the subdomain Ψ in the current design domain can be calculated by the same procedure to calculate $\mathbf{k}_e^{\Omega}$ of the subdomain Ω in the initial design domain.

If all element stiffness matrices $\mathbf{k}_e^{C}$ are computed in current design C, the global stiffness matrix can be assembled using Eq. (2.3). Although the entire domain is divided in to a set of subdomains, the problem is solved entirely rather than partially. Thus, this method is named Domain Composition Method (DCM).

2.3. Domain Composition Optimization

In this section, the static analysis using domain composition method is applied in structural optimization to design optimal structures. Strain energy based optimization problems are formulated and the sensitivities of two types of design variables, material distribution variables and scaling factors, are derived.

2.3.1. Problem Formulation

A strain energy based formulation is considered in this work. Strain energy is the potential energy stored in a structure, and it is balanced with the work done by external load in an elastic material. It is defined as

$$U = \int_V \boldsymbol{\sigma}^T \boldsymbol{\varepsilon} dV \tag{2.16}$$

where $\boldsymbol{\sigma}$ denotes the stress tensor and $\boldsymbol{\varepsilon}$ denotes the strain tensor.

In finite element analysis, Eq. (2.16) is discretized as

$$U = \frac{1}{2}\mathbf{u}^T\mathbf{F} = \frac{1}{2}\mathbf{u}^T\mathbf{K}\mathbf{u} = \sum_{e=1}^{N}\frac{1}{2}\mathbf{u}_e^T\mathbf{k}_e\mathbf{u}_e \tag{2.17}$$

where N is the number of elements in volume V. $\mathbf{k}_e$ and $\mathbf{u}_e$ are the element stiffness matrix and the element nodal displacement vector, respectively. The strain energy function is one of the comprehensive indicators to measure the structure deformation.

In structural optimization, compliance is used more widely as the objective function. It is equivalent to the strain energy function, only without the coefficient $1/2$ in front of the strain energy. Compliance is defined as

$$C = \mathbf{u}^T \mathbf{F} = \mathbf{u}^T \mathbf{K} \mathbf{u} \tag{2.18}$$

In this dissertation, the strain energy function is used because it gives a clear physical meaning than compliance.

Using the previous example demonstrates the design domain in Figure 2.6, the formulation can be extended as general form. This example gives the initial design I and scaling factors defined in different subdomains. In current design C, a total strain energy objective function with the constant volume constraint, using static analysis, a structural optimization problem is formulated as

$$\begin{aligned} &\underset{\gamma,\lambda}{Min}: \; U_T^C = \frac{1}{2} \mathbf{u}^{CT} \mathbf{K}^C \mathbf{u}^C \\ &s.t.: \quad \mathbf{K}^C \mathbf{u}^C = \mathbf{F} \\ &\qquad V^C(\boldsymbol{\gamma}, \boldsymbol{\lambda}) \le \overline{V} \\ &\qquad 0 < \gamma_{\min} \le \gamma_i \le 1, \;\; i = 1, \cdots, N \\ &\qquad 0 < \underline{\lambda}_j \le \lambda_j \le \overline{\lambda}_j, \;\; j = 1, \cdots, M \end{aligned} \tag{2.19}$$

where $\overline{V}$ is the upper bound of the volume which is predefined by the designer. N is the total number of elements in the entire domain. M is the number of scaling factors describing dimensions in different subdomains.

In the optimization problem, two types of design variables are considered: (1) material distribution variables, i.e. element pseudo-densities $\boldsymbol{\gamma}$, which defined in SIMP model and (2) shape variables, i.e. the scaling factors $\boldsymbol{\lambda}$, which defined in Section 2.2.2. They are all bounded by specified upper and lower bounds to guarantee that the problem is a well-bounded optimization problem.

The constant volume constraint is considered in the optimization problem. The constant volume constraint requires the total material volume is kept at a constant value, and it does not change even when the size of the entire design domain varies.

2.3.2. Sensitivity Analysis

In order to solve the structural optimization problem as Eq. (2.19), the gradient-based mathematical optimization algorithm is needed. The gradient information is always called sensitivity in structural optimization filed. There are two types of the sensitivities for two types of design variables: the material distribution variable and the shape variable.

The sensitivity of the material distribution variable is consistent with the traditional topology optimization because the material distribution variable γ_i is only related to the material property, and it is not affected by the shape variables.

Taking derivative of the static equilibrium equation with respect to the material distribution variable γ_i

$$\frac{\partial \mathbf{K}^C}{\partial \gamma_i}\mathbf{u}^C + \mathbf{K}^C \frac{\partial \mathbf{u}^C}{\partial \gamma_i} = \mathbf{0} \tag{2.20}$$

where $\partial \mathbf{F} / \partial \lambda_j = \mathbf{0}$ for a design independent load. The derivative to the total strain energy is

$$\frac{\partial U_T^C}{\partial \gamma_i} = \frac{1}{2}\mathbf{u}^{CT} \frac{\partial \mathbf{K}^C}{\partial \gamma_i}\mathbf{u}^C + \mathbf{u}^{CT}\mathbf{K}^C \frac{\partial \mathbf{u}^C}{\partial \gamma_i} \tag{2.21}$$

Substituting Eq. (2.20) into Eq. (2.21), it obtains

$$\frac{\partial U_T^C}{\partial \gamma_i} = -\frac{1}{2}\mathbf{u}^{CT}\frac{\partial \mathbf{K}^C}{\partial \gamma_i}\mathbf{u}^C = -\frac{p}{\gamma_i}\frac{1}{2}\mathbf{u}_e^T\mathbf{k}_e\mathbf{u}_e = -\frac{p}{\gamma_i}U_i^C \tag{2.22}$$

where p is the penalty coefficient to material from SIMP model. U_i^C is the element strain energy of the i^{th} element and it can be calculate easily from element stiffness **v** matrices and displacement vector.

The calculation of the sensitivity of the shape variable will be presented in this section. It can be derived using the adjoint method. A Lagrange multiplier vector is introduced, and the modified objective function can be written as

$$U_T^C = \frac{1}{2}\mathbf{u}^{CT}\mathbf{K}^C\mathbf{u}^C + \mathbf{v}^{CT}\left(\mathbf{F} - \mathbf{K}^C\mathbf{u}^C\right) \tag{2.23}$$

where the second part of the modified objective function is equal to zero and is equivalent to U_T^C.

Taking derivative of the new objective function w.r.t. λ_j, and setting the adjoint displacement as

$$\mathbf{v}^C = \mathbf{u}^C \tag{2.24}$$

For a design independent load, it has $\partial\mathbf{F}/\partial\lambda_j = \mathbf{0}$, and then it gives

$$\frac{\partial U_T^C}{\partial \lambda_j} = -\frac{1}{2}\mathbf{u}^{CT}\frac{\partial \mathbf{K}^C}{\partial \lambda_j}\mathbf{u}^C \tag{2.25}$$

From Eq. (2.25), the partial derivative term is not easy to evaluate because the shape variable λ_j is related to some subdomains affect by this variable. However, it can be decomposed into element level terms as

$$\frac{\partial U_T^C}{\partial \lambda_j} = -\frac{1}{2}\mathbf{u}^{CT}\frac{\partial \mathbf{K}^C}{\partial \lambda_j}\mathbf{u}^C = -\sum_{e\in C}\left(\frac{1}{2}\mathbf{u}_e^{CT}\frac{\partial \mathbf{k}_e^C}{\partial \lambda_j}\mathbf{u}_e^C\right) \tag{2.26}$$

where $\mathbf{k}_e^C$, $\mathbf{u}_e^C$ are element stiffness matrix and element nodal displacement vector of current design C.

If the sensitivity of the element stiffness matrix $\mathbf{k}_e^C$ w.r.t. λ_j is considered in arbitrary subdomain Ψ, it has $\mathbf{k}_e^C = \mathbf{k}_e^\Psi$ and gives following results from Eq. (2.14):

(1) If $\lambda_j = \lambda_{jx}$ or λ_{jy}

$$\frac{\partial \mathbf{k}_e^\Psi}{\partial \lambda_j} = \int_{-1}^{1}\int_{-1}^{1}\left[\mathbf{N_D}^T\mathbf{T}^{\Omega T}\left(\frac{\partial \mathbf{A}'}{\partial \lambda_j}\right)^T\mathbf{E}\mathbf{A}'\mathbf{T}^\Omega\mathbf{N_D} + \mathbf{N_D}^T\mathbf{T}^{\Omega T}\mathbf{A}'^T\mathbf{E}\left(\frac{\partial \mathbf{A}'}{\partial \lambda_j}\right)\mathbf{T}^\Omega\mathbf{N_D}\right]J^\Omega d\xi d\eta \tag{2.27}$$

where

$$\frac{\partial \mathbf{A}'}{\partial \lambda_{jx}} = -\frac{1}{2\sqrt{\lambda_{jx}\lambda_{jy}}}\begin{bmatrix}\lambda_{jy}/\lambda_{jx} & 0 & 0 & 0\\ 0 & 0 & 0 & -1\\ 0 & -1 & \lambda_{jy}/\lambda_{jx} & 0\end{bmatrix} \text{ if } \lambda_j = \lambda_{jx}, \text{ and}$$

$$\frac{\partial \mathbf{A}'}{\partial \lambda_{jy}} = -\frac{1}{2\sqrt{\lambda_{jx}\lambda_{jy}}}\begin{bmatrix}-1 & 0 & 0 & 0\\ 0 & 0 & 0 & \lambda_{jx}/\lambda_{jy}\\ 0 & \lambda_{jx}/\lambda_{jy} & -1 & 0\end{bmatrix} \text{ if } \lambda_j = \lambda_{jy}$$

(2) If $\lambda_j \neq \lambda_{jx}$ or λ_{jy}, i.e. λ_j is not related to this element

$$\frac{\partial \mathbf{k}_e^\Psi}{\partial \lambda_j} = \mathbf{0} \tag{2.28}$$

Thus, $\partial \mathbf{k}_e^{\Psi} / \partial \lambda_j$ can be computed as a separated routine and combined in the static analysis, and then the sensitivity $\partial U_T^C / \partial \lambda_j$ can be evaluated.

2.4. Numerical Examples

2.4.1. Package Cushioning Design: Total Strain Energy Formulation

In this section, the first example is the static version of the package cushioning design problem which is considered in the discussion of Domain Composition Method (DCM) and it is compared with conventional topology optimization design. As shown in Figure 2.7, this example is to find the optimal cushioning structure under static loads and the total strain energy formulation as shown in Eq. (2.19) is employed.

In this example, the initial configuration is displayed in Figure 2.7. The content is located at the center of the rectangular domain and the cushioning design domain is symmetric. The outside cushioning area is designable and the inside content area is non-designable, i.e. it keeps unchanged in optimization process. The initial configuration is modeled as the upper bounds of all thicknesses of cushioning. The top edge is assumed fixed and a left bottom corner load $F = 1414\ kN$ is applied. The material properties are set as follows: For the content: Young's modulus $E_0 = 20\ GPa$, Poisson's ratio $\nu = 0.3$; and for the design domain: Young's modulus $E_0 = 0.2\ GPa$, Poisson's ratio $\nu = 0.3$. It shows that the soft cushioning material protects the stiff content. Volume constraint is set as 30% of the initial design cushioning volume and the design domain is meshed by four node quadrilateral (Q4) elements.

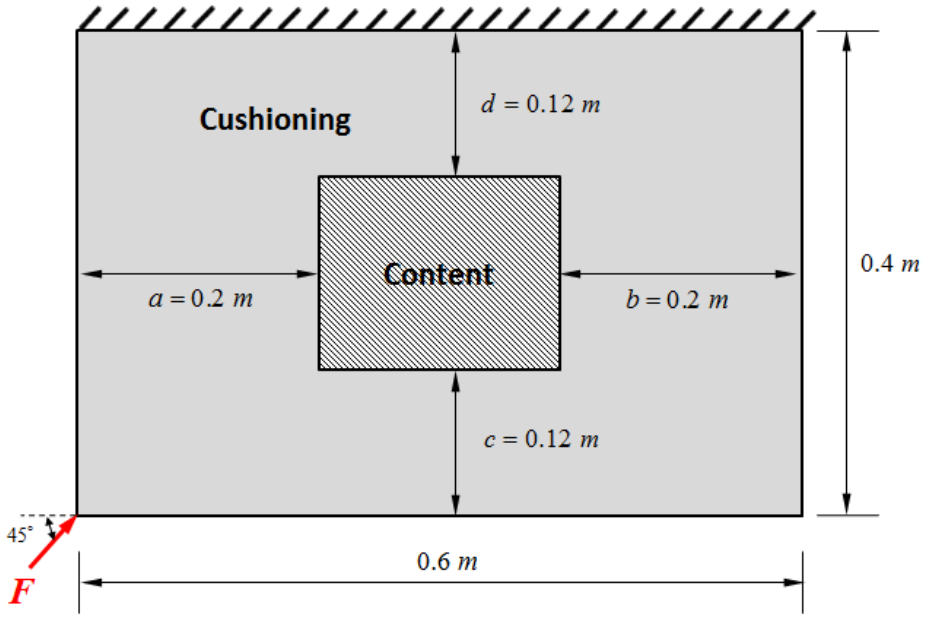

Figure 2.7. Example of Static Version of Cushioning Design

Three cases are considered and their results are shown in Figure 2.8. All cases employ the total strain energy formulation and two symmetric boundary conditions. Case 1 is the conventional topology optimization result and it is treated as comparison purpose, i.e. the cushioning design domain is fixed as initial configuration. Case 2 is the result of DCM with bounded length and fixed height of design domain. Case 3 is the result of DCM with bounded length and height of design domain. The lower and upper bounds of the cushioning dimensions, the optimal cushioning dimensions and the optimal total strain energy are listed in Table 2.1.

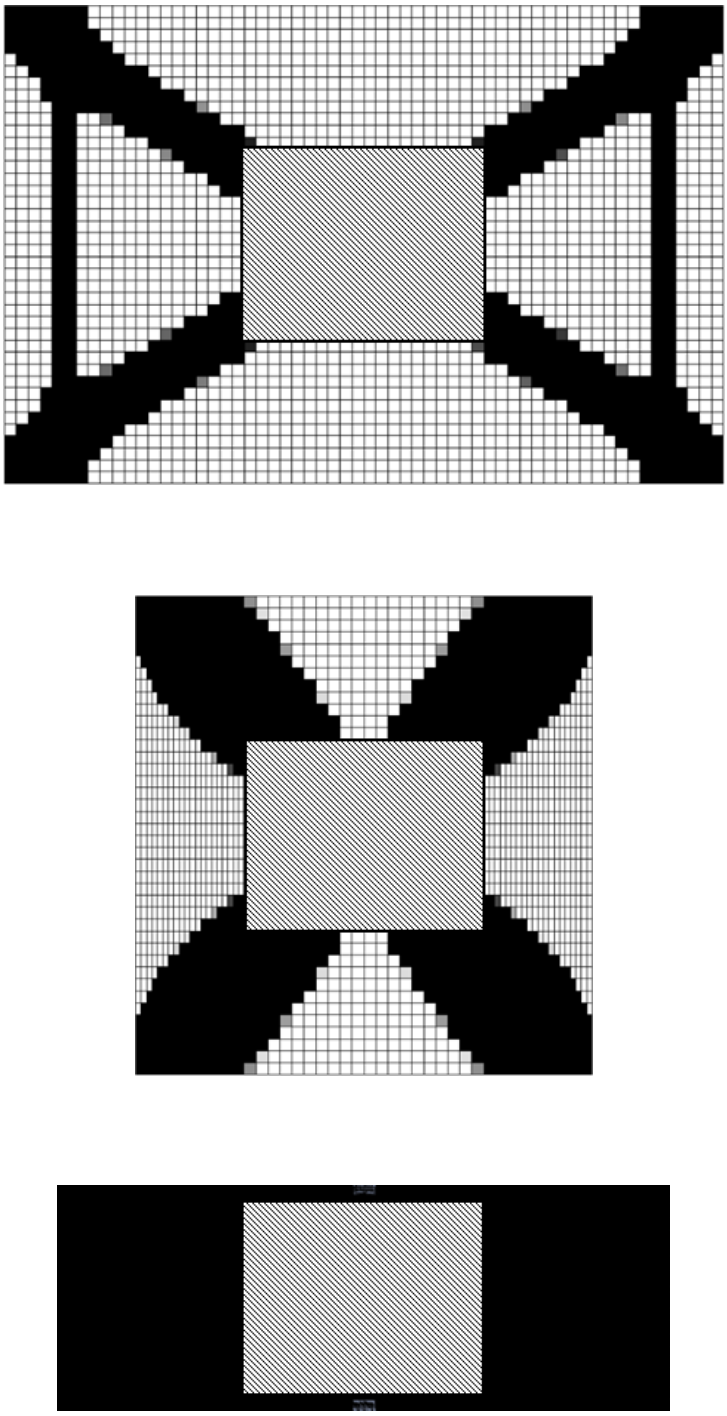

Figure 2.8. Cushioning Design Cases: Case 1. Conventional Topology Optimization (Top), Case 2. DCM with Bounded Length and Fixed Height (Middle), Case 3. DCM with Bounded Length and Height (Bottom)

Table 2.1. Comparison of Three Results for Package Cushioning Design

Cases	Bounds of Cushioning	Optimal Dimensions of Cushioning	Optimal Total Strain Energy
Case 1: Conventional Topology Optimization	a, b, c, d are fixed	$a = 0.2$ $b = 0.2$ $c = 0.12$ $d = 0.12$	48076.1079
Case 2: DCM with Bounded Length and Fixed Height	$a, b \in [0.02, 0.2]$ c, d are fixed	$a^* = 0.09$ $b^* = 0.09$ $c = 0.12$ $d = 0.12$	29333.2039
Case 3: DCM with Bounded Length and Height	$a, b \in [0.02, 0.2]$ $c, d \in [0.012, 0.12]$	$a^* = 0.153$ $b^* = 0.153$ $c^* = 0.012$ $d^* = 0.012$	21062.1520

In Table 2.1, the dimensions of cushioning are different. In Case 1, length and height of the cushioning are fixed and it gives the greatest value of the total strain energy of the whole structure. In Case 2, height of the cushioning is fixed and length obtains the optimal value between the lower and upper bounds of given. In Case 3, length and height of the cushioning are bounded by predefined bounds. The heights reach the lower bounds and the lengths converge to the optimal values. The optimal total strain energy values decrease from Case 1 to Case 3. To present the structural deformations, strain energy distributions of the optimal designs are shown in Figure 2.8 and all cases are plotted in the same contour legend range. Case 2 and 3 show smaller strain energy distributions than Case 1 and it is consistent with the total strain energy results in Table 2.1.

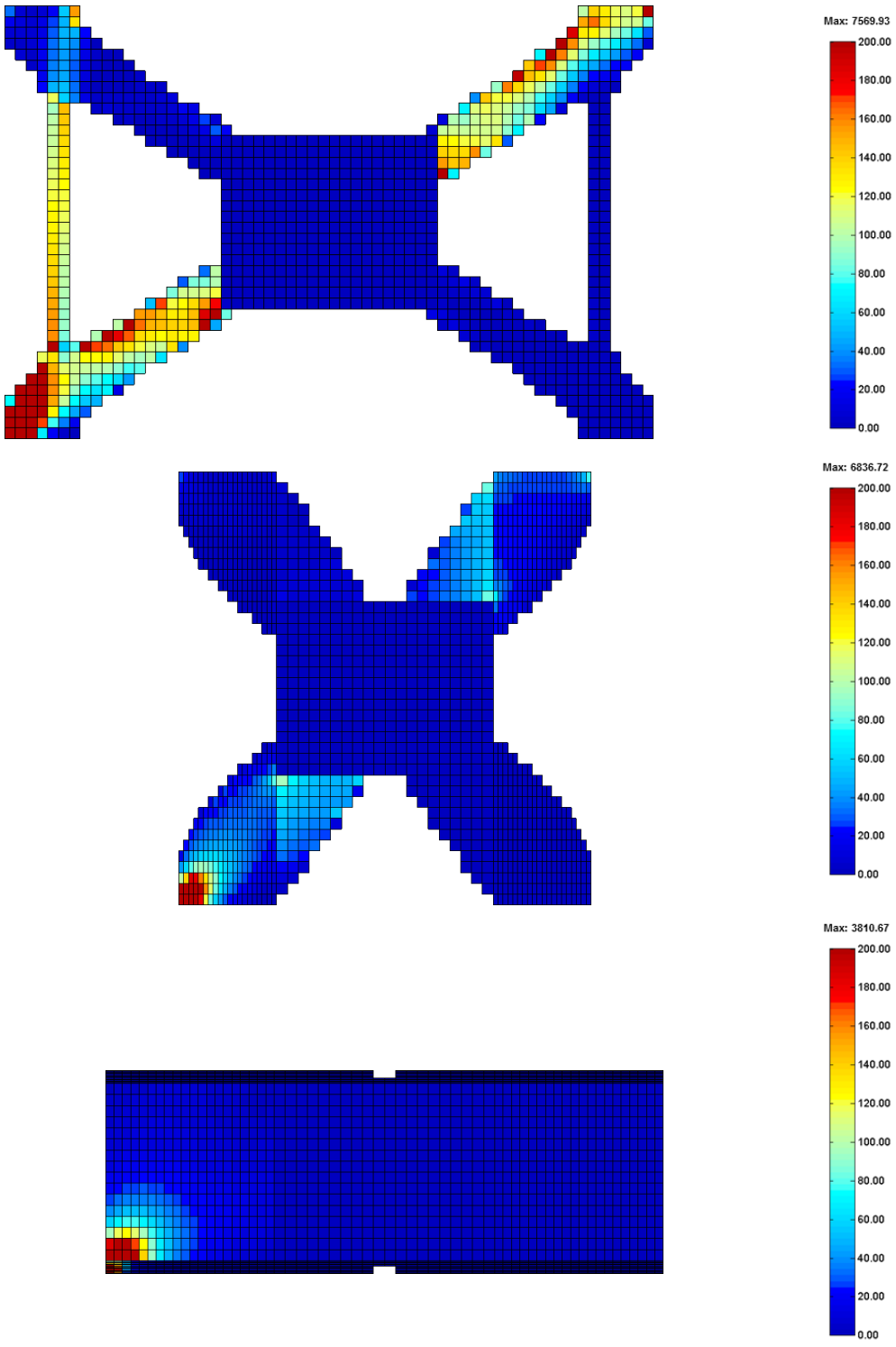

Figure 2.9. Strain Energy Distributions of Cushioning Design Cases: Case 1. Conventional Topology Optimization (Top), Case 2. DCM with Bounded Length and Fixed Height (Middle), Case 3. DCM with Bounded Length and Height (Bottom)

This example demonstrates the effectiveness of DCM. The optimal objective function value, i.e. total strain energy, is reduced in Case 2 and Case 3 comparing with Case 1, so DCM give better solutions than conventional topology optimization method.

2.4.2. Cantilever Beam with a Movable Hole Design

The former example changes the size of design domain. However, application of DCM is not restricted here and it is possible adjust the boundary of design domain. A cantilever beam with a movable hole example is studied as follows. It is a simplification of the real design problem. In the wings of the airplane, ribs support the airfoil shape of the wings and attach to the main spar. In order to reduce the weight of the wings, topology optimization is applied and the holes are generated in the design domain. Some lines and pipes pass through the ribs so the holes have the lower bounds. However, the location of the predefined hole is not fixed and it gives the different topology of the rib structure. Proposed DCM using total strain energy formulation can be applied in this problem.

The problem is considered as a short cantilever beam and the initial design is shown in Figure 2.10. This beam is fixed at the left edge and the external force $F = 100kN$ is applied downward at the bottom right corner. The following elastic material properties are assumed: Young's modulus $E_0 = 206GPa$, Poisson's ratio $\nu = 0.3$. The 50% of the total design volume is applied as the bound of the volume constraint. The design domain is meshed by four node quadrilateral (Q4) elements. The center of the circular hole is located at $(0.6,\ 0.3)$, i.e. at the middle of length and width initially. The design composition which is applied in this example is shown as Figure 2.11.

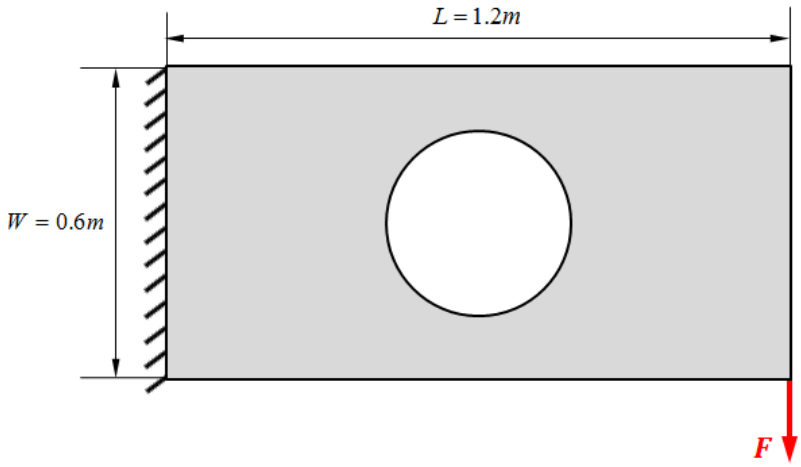

Figure 2.10. Initial Design Domain and Hole Location of Example 1

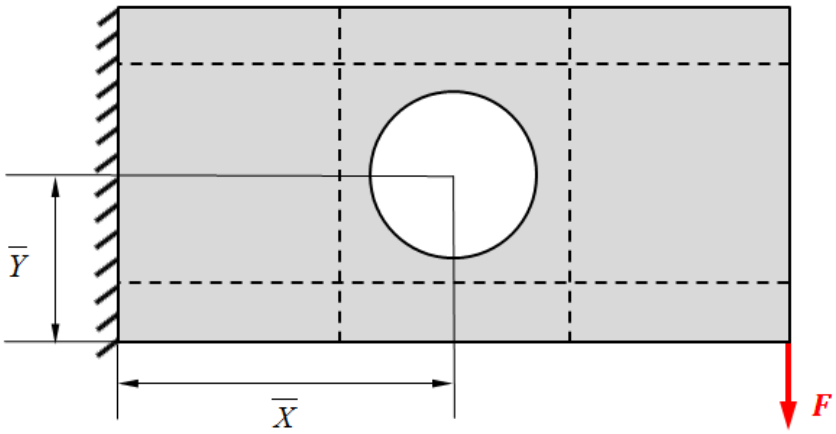

Figure 2.11. Initial Design Domain Composition

The design objective is to generate the most rigid structure and find the optimal location of the circular hole under the volume constraint. Four cases are shown from Figure 2.12 to Figure 2.15. Case 1 to Case 3 is the result of topology optimization using total strain energy formulation and the different locations of the center of the hole for comparison purposes: Case 1 is located at $(L/3,\ W/2)$; Case 2 is located at $(L/2,\ W/2)$;

and Case 3 is located at $(2L/3,\ W/2)$. Case 4 is the result of DCM using total strain energy formulation with small height and width lower bounds which is formulated as Eq. (2.19). The lower bounds and upper bounds of length and width, the optimal location of the center of circular hole and the optimal total strain energy of beam are listed in Table 2.2.

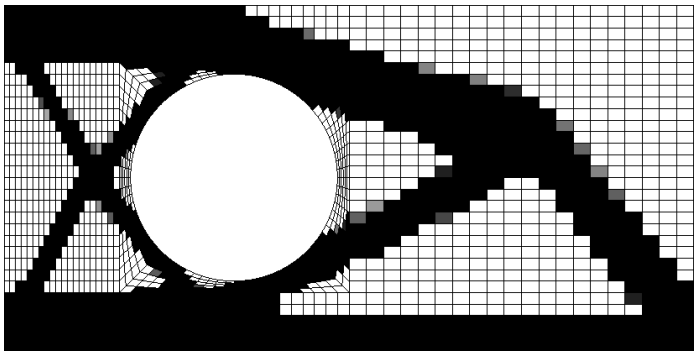

Figure 2.12. Optimal Material Distribution for Fixed Hole Location $(L/3,\ W/2)$

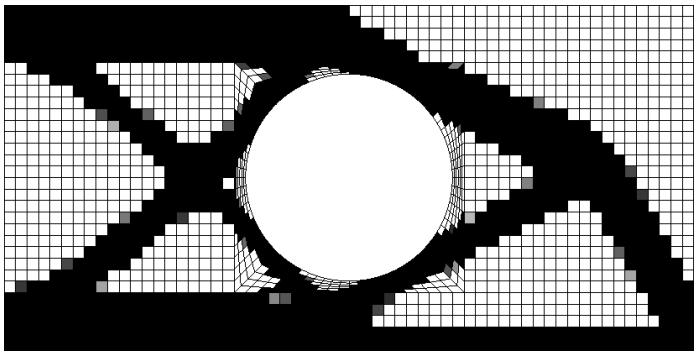

Figure 2.13. Optimal Material Distribution for Fixed Hole Location $(L/2,\ W/2)$

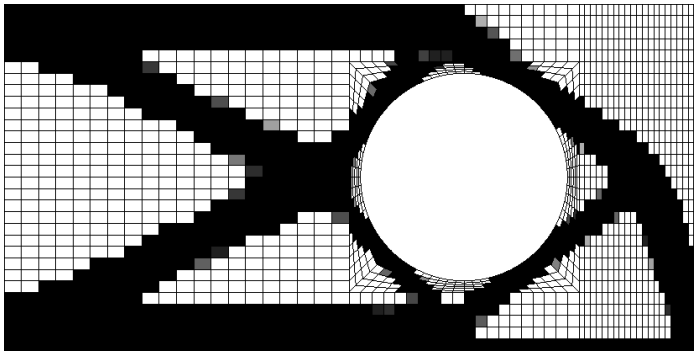

Figure 2.14. Optimal Material Distribution for Fixed Hole Location $(2L/3,\ W/2)$

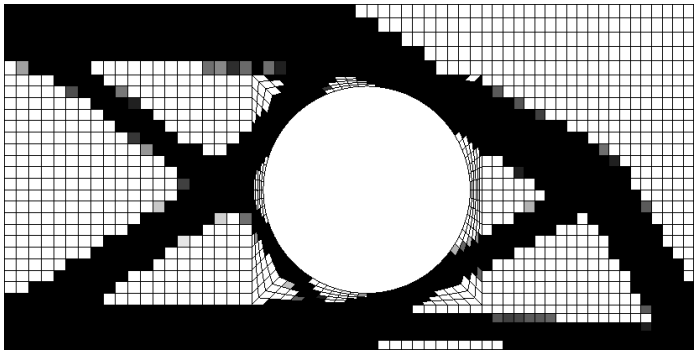

Figure 2.15. Optimal Material Distribution and Optimal Hole Location

Table 2.2. Comparison of Results for Cantilever Beam with a Movable Hole Design

Cases	Bounds of Location of Center of the Circular Hole	Optimal Location of Center of the Circular Hole	Total Strain Energy
Case 1: Topology Optimization using Total Strain Energy	$\bar{X}, \bar{Y}$ are fixed	$\bar{X} = 0.4$ $\bar{Y} = 0.3$	206.0635
Case 2: Topology Optimization using Total Strain Energy	$\bar{X}, \bar{Y}$ are fixed	$\bar{X} = 0.6$ $\bar{Y} = 0.3$	196.3870

Case 3: Topology Optimization using Total Strain Energy	$\bar{X}, \bar{Y}$ are fixed	$\bar{X} = 0.8$ $\bar{Y} = 0.3$	201.4163
Case 4: DCM using Total Strain Energy	$\bar{X} \in [0.4, 0.8]$ $\bar{Y} \in [0.2, 0.4]$	$\bar{X}^* = 0.6528$ $\bar{Y}^* = 0.2813$	195.7394

In Table 2.2, the optimal objective function value in Case 4, i.e. the total strain energy of the beam, is smallest than the values in difference location cases. Case 2 also gives a small value of the objective function because the center of location of circular hole is close to the optimal solution. The differences of the objective function values are small because the bending configuration is not very sensitive to the location of the holes in this problem. This example shows that the DCM can be extended to solve the design domain boundary change problem.

2.5. Conclusion and Remark

In this chapter, Domain Composition Method (DCM) is presented and discussed. First of all, the fixed design domain in topology optimization is studied and it is selected based on a prior knowledge of designer. However, if designer has flexibility to change whole or a partial of the design domain, it might be got a better solution. The conventional topology optimization is challenging to handle this kind of problem.

To change the design domain, the parameterization is needed. A straightforward parameterization is direct dimensions. However, this method is difficult to be combined into the existing topology optimization procedure because the sensitivity of the

parameters cannot be derived analytically. The finite difference method to calculate the sensitivity which was applied has some obvious drawbacks.

To avoid these drawbacks, DCM is proposed. At the beginning, the entire design domain is divided into several subdomains. A set of scaling factors is defined to parameterize the subdomains' change between the initial design and the current design which is termed subdomain transformation. An example is used to demonstrate the new parameterization will not increase the number of variable. The concept of DCM is applied in linear elastic static analysis and then integrated into the strain energy based structure optimization problem. In order to solve this optimization problem using the gradient-based mathematical optimization algorithm, the sensitivities of two kinds of design variables, the material distribution variable and the scaling factors, are derived respectively. Unlike the topology optimization, domain composition optimization is not only distributing material between elements but also trade off material between different subdomains because of the change of subdomains. Two numerical examples: one package cushioning design under static load problem demonstrates the effectiveness of DCM; another one cantilever beam with a movable hole design problem presents the extension of DCM to solve the boundary change problem.

Finally, it is worth to note that DCM can be not only integrated in static analysis, but also applied in a lot of other physics for structural optimization problem, such as dynamic analysis, electromagnetics, acoustic and vibration.

Chapter 3. Domain Composition Method (DCM) using Regional Strain Energy Formulation

DCM is developed and is applied in structural optimization problem in Chapter 2 which the total strain energy is used as the objective function. This chapter focuses on the protective structure design. A regional strain energy formulation is discussed and applied in the protective structure design. The structural optimization problem is formulated using DCM and its sensitivities are derived for two types of variables.

3.1. Protective Structure and Total Strain Energy Formulation

Protective structure is a type of structure to protect the content which is easy broken or fragile. The protective structures include the civil structure, vehicle white body, bridge infrastructure, ship frame and packaging cushioning. The functions of the protective structure are hold, support or protect the content or space. A typical protective structure is a package cushioning structure, it protect the inside content. Cushioning controls shock and vibration in storage and transportation process and reduces the chance of product damage. The outside box contains the cushion and the inside content.

Obviously, proper performance of cushioning is dependent on its proper design and use, and then how to design the cushioning is a typical engineering problem. A good protective cushioning can be considered from two aspects: the inside content is well-protected and the cushioning material is reduced.

There are two ways to reduce the cushioning briefly. One is reducing the cushioning material and another one is shrinking the size of packaging (including cushion and box). Reducing material from the cushioning structure declines material and weight

of packaging. Shrinking the size of cushioning reduces the volume and weight in storage, transportation, delivery and recycling. It saves money in the packaging life cycle and provides better protection for the inside content. It satisfies the requirement from economical and sustainable perspectives in current industries.

Total strain energy formulation is not good for the protective structure because the total strain energy of the structure is decreased is not equivalent to the strain energy of protected content is decreased. In contrast, strain energy might be pushed from the protective structure design domain to the protected content. It does not match the design target to minimize the deformation of the protected content. To overcome this dilemma, a regional strain energy formulation is proposed in this chapter.

3.2. Regional Strain Energy Formulation for DCM

3.2.1. Problem Formulation

In Chapter 2, DCM is proposed and the entire domain is divided into several subdomains and each subdomain changes between the initial design and the current design based on the subdomain transformation.

Correspondingly, strain energy is parted into the different subdomains. Naturally, it can be extended as regional strain energy. The “region” is naturally defined as a set of subdomains. Strain energy is distributed between the different subdomains. However, region and subdomain are different and they are defined in different perspective. The region is defined from objective function perspective. To satisfy the objective requirement, the design domain is separated into different regions and the objective function is defined for different regions. The subdomain is defined in design domain

perspective. A region is a group of server subdomains or a partial of a subdomain. They are used in different context.

In Chapter 2, total strain energy based structure optimization problem is proposed. In this formulation, the entire design domain is treated as a whole and the objective function is the strain energy of the whole design domain. The whole structure strain energy is considered as a comprehensive measurement of the whole structure deformation. However, a special region is required to be emphasized or to avoid of the strain energy concentration. For example, a region in the entire domain is very sensitive for strain energy concentration, or a region need protection, a region absorb more strain energy and so on. The objective function should include regional strain energy which stores in the different regions. If the entire domain is separated into several regions, the objective function can be considered as a certain combination with these regions. That's reason regional strain energy formulation is needed. Gea [51] proposed the concept of regional strain energy and applied it in energy absorption design. This concept is extended to the generalized topology optimization proposed in this chapter.

The package cushioning is a typical protective structure. The simplified 2D cushioning example is shown in Figure 3.1. The shadowed region demonstrates the protected content. The design domain is the region outside of the content. The design target is to find the protective structure that provides the best protection for the content. The proposed method to solve the problem also can be used to design other protective structures such as vehicles and electronics devices.

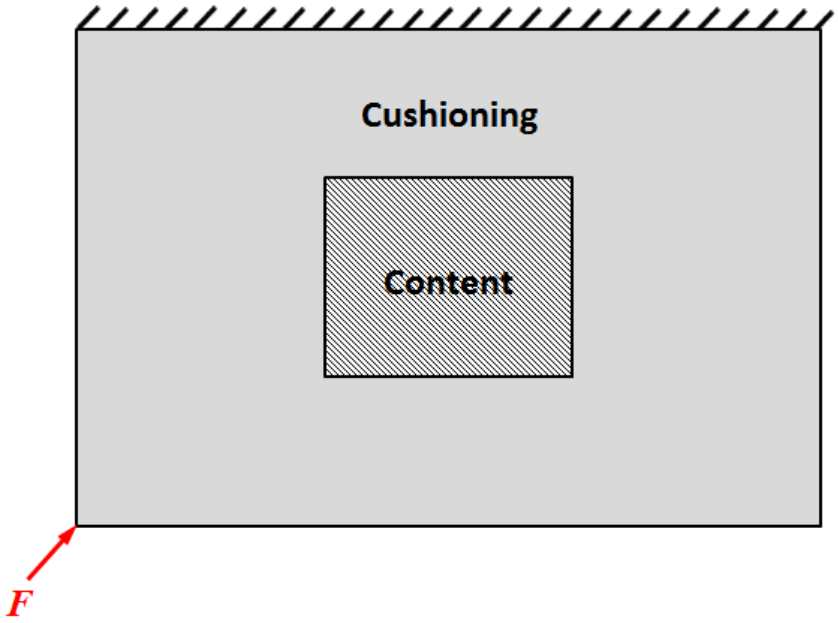

Figure 3.1. Initial Design of Cushioning Design Example

In this example, the inside content is non-designable region and the outside region is designable region. The design target is considered as: the content is well protected and a protective structure is generated under the limited material constraint. It can be interpreted as: the objective is to minimize the strain energy imposed in the content, rather than to minimize the total strain energy in the whole structure because the content is our design focus. However, the structural integrity in the protective structure design domain should be maintained. There are two objectives need to be satisfied in our design problem: minimize the strain energy in the protected content and minimize the strain energy in the protective design domain. Thus, it is a multi-objective design problem.

There are a lot of different methods were proposed to convert a multi-objective problem to a single-objective design problem [66], a simple conversion is chosen in our

research. A new objective function based on regional strain energy concept is proposed for protective structure design

$$U_R \cdot U_T \tag{3.1}$$

where U_R denotes the strain energy generated in content and U_T denotes the total strain energy produced in the whole structure design domain. This is a straightforward selection because the design target is minimizing two objectives simultaneously.

In previous chapter, DCM is proposed and the entire domain is divided into subdomains. It is intuitively to connect the protective structure design with DCM. It is possible to get a better design if the design domain is possible to change. The protective structure design problem using DCM is formulated as

$$\begin{aligned} &\underset{\boldsymbol{\gamma},\boldsymbol{\lambda}}{Min}: \ U_R^C \cdot U_T^C \\ &s.t.: \quad \mathbf{K}^C\mathbf{u}^C = \mathbf{F} \\ &\qquad V^C\left(\boldsymbol{\gamma},\boldsymbol{\lambda}\right) \le \overline{V} \\ &\qquad 0 < \gamma_{\min} \le \gamma_i \le 1, \ \ i = 1,\cdots,N \\ &\qquad 0 < \underline{\lambda}_j \le \lambda_j \le \overline{\lambda}_j, \ \ j = 1,\cdots,M \end{aligned} \tag{3.2}$$

where $\overline{V}$ is the volume upper bound which is predefined by designer. N is the element number in design domain. M is the number of scaling factors which are defined in different subdomains.

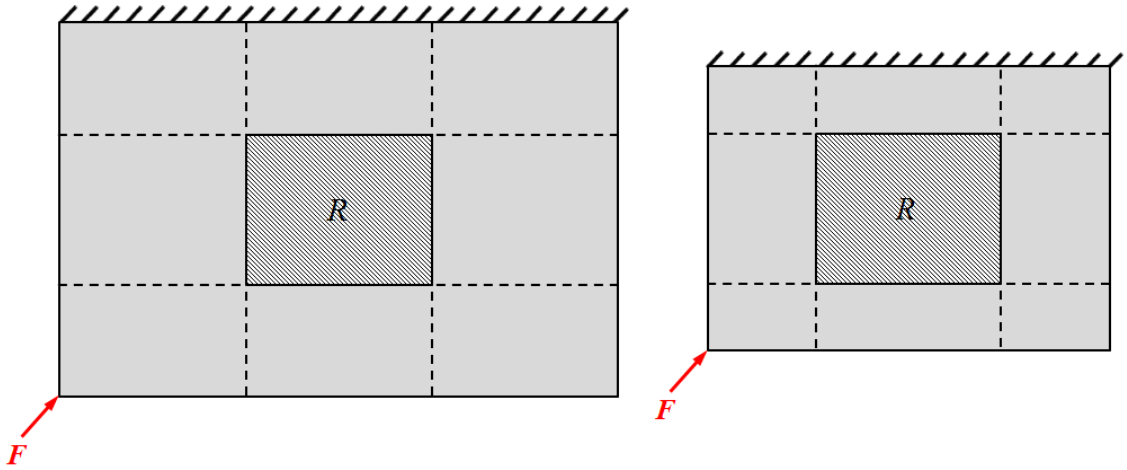

Figure 3.2. Region R and Domain Decomposition

In the topology optimization problem stated in Eq. (3.2), U_R^C is the strain energy of the content region in current design C and U_T^C is the total strain energy of whole structure in current design C. The material of the content might be harder or softer material compared with material which is assigned to the design domain. Inside content is non-designable region and the content is predefined by user and does not change in the protective structure design process.

Additionally, it is worth to note the problem defined in Eq. (3.2) can be applied not only to protective structure design but also to support structure design. This extended application is illustrated by a numerical example in this chapter.

3.2.2. Sensitivity Analysis

To solve the optimization problem Eq. (3.2), the sensitivity analysis is required. Two types of design variables exist if DCM is applied: material distribution design variable γ_i and shape variable λ_j and their sensitivity derivation is similar. The

derivation of the sensitivity w.r.t. the shape variable λ_j is discussed as follows and the sensitivity w.r.t. the material distribution variable γ_i is revised from the similar derivation process. Their results are given separately.

In the objective function of the optimization problem Eq. (3.2), the strain energy in content region U_R^C and the total strain energy in entire domain U_T^C can be evaluated from the static analysis.

From the chain rule for the derivative w.r.t the shape variable λ_j, it gives

$$\frac{\partial\left(U_R^C \cdot U_T^C\right)}{\partial\lambda_j} = \frac{\partial U_R^C}{\partial\lambda_j} U_T^C + \frac{\partial U_T^C}{\partial\lambda_j} U_R^C \tag{3.3}$$

The sensitivity of total strain energy $\partial U_T^C / \partial\lambda_j$ has the same result as Eq. (2.22) and only the sensitivity $\partial U_R^C / \partial\lambda_j$ need to be derived. To derive the sensitivity of the regional strain energy U_R^C, the adjoint method is applied, and a Lagrange multiplier vector $\mathbf{v}^{\Psi}$ is introduced. The objective function in Eq. (3.2) is rewritten as

$$U_R^C = \sum_{q\in R} \frac{1}{2} \mathbf{u}_q^{CT} \mathbf{k}_q^C \mathbf{u}_q^C + \mathbf{v}^{CT}\left(\mathbf{F} - \mathbf{K}^C \mathbf{u}^C\right) \tag{3.4}$$

where the second term is equal to zero. Taking derivative to the new objective function w.r.t. λ_j yields

$$\frac{\partial U_R^C}{\partial\lambda_j} = \sum_{q\in R} \frac{1}{2} \mathbf{u}_q^{CT} \frac{\partial \mathbf{k}_q^C}{\partial\lambda_j} \mathbf{u}_q^C + \sum_{q\in R} \mathbf{u}_q^{CT} \mathbf{k}_q^C \frac{\partial \mathbf{u}_q^C}{\partial\lambda_j} + \mathbf{v}^{CT}\left(\frac{\partial \mathbf{F}}{\partial\lambda_j} - \frac{\partial \mathbf{K}^C}{\partial\lambda_j}\mathbf{u}^C - \mathbf{K}^C \frac{\partial \mathbf{u}^C}{\partial\lambda_j}\right) \tag{3.5}$$

For a design independent load, it has $\partial \mathbf{F}/\partial \lambda_j = \mathbf{0}$. To eliminate the unknown $\partial \mathbf{u}_q^C/\partial \lambda_j$ and $\partial \mathbf{u}^C/\partial \lambda_j$ from the sensitivity expression for the structure, vector $\mathbf{v}^C$ is given from the following equation

$$\left(\frac{\partial \mathbf{u}^C}{\partial \lambda_j}\right)^T \left(\mathbf{K}^C \mathbf{v}^C - \mathbf{K}_R^C \mathbf{u}_R^C\right) = 0 \tag{3.6}$$

where $\mathbf{K}_R^C$ and $\mathbf{u}_R^C$ are assembled element stiffness matrix and element nodal displacement, which has the same dimension as the total number of DOFs. Only those nodes which belong to domain R will give non-zero values in $\mathbf{K}_R^C$ and $\mathbf{u}_R^C$. One possible solution is

$$\mathbf{K}^C \mathbf{v}^C = \mathbf{K}_R^C \mathbf{u}_R^C \tag{3.7}$$

The adjoint vector $\mathbf{v}^C$ can be calculated from this equation. The applied force vector is the right hand side term $\mathbf{K}_R^C \mathbf{u}_R^C$, and it can be obtained as the elemental nodal forces from the static analysis.

Eq. (3.5) can be simplified as follows by applying Eq. (3.6)

$$\frac{\partial U_C^\Psi}{\partial \lambda_j} = \sum_{q \in C} \frac{1}{2} \mathbf{u}_q^{\Psi T} \frac{\partial \mathbf{k}_q^\Psi}{\partial \lambda_j} \mathbf{u}_q^\Psi - \mathbf{v}^{\Psi T} \frac{\partial \mathbf{K}^\Psi}{\partial \lambda_j} \mathbf{u}^\Psi \tag{3.8}$$

The above sensitivity can be evaluated by applying Eq. (2.27) and (2.28).

The sensitivity w.r.t. the material distribution variable γ_i has the similar derivation from Eq. (3.3) to (3.8). As Eq. (3.3), The chain rule for the derivative w.r.t the material distribution variable γ_i, it gives

$$\frac{\partial\left(U_R^C \cdot U_T^C\right)}{\partial \gamma_i} = \frac{\partial U_R^C}{\partial \gamma_i} U_T^C + \frac{\partial U_T^C}{\partial \gamma_i} U_R^C \tag{3.9}$$

The total strain energy derivative $\partial U_T^C / \partial \gamma_i$ is same as Eq. (2.22) and only the derivative $\partial U_R^C / \partial \gamma_i$ in Eq. (3.3) is to be derived. The same adjoint vector $\mathbf{v}^C$ from Eq. (3.7) is applied and no additional adjoint analysis is needed. The result is directly given

$$\frac{\partial U_R^C}{\partial \gamma_i} = \sum_{q \in R} \frac{1}{2} \mathbf{u}_q^{CT} \frac{\partial \mathbf{k}_q^C}{\partial \gamma_i} \mathbf{u}_q^C - \mathbf{v}^{CT} \frac{\partial \mathbf{K}^C}{\partial \gamma_i} \mathbf{u}^C \tag{3.10}$$

Because the material distribution variable γ_i is only related to the ith element of the domain, the result can be simplified when SIMP model is applied.

(1) If i^{th} element is outside to the region R, the first term is equal to zero.

$$\frac{\partial U_R^C}{\partial \gamma_i} = -\mathbf{v}_i^{CT} \frac{\partial \mathbf{k}_i^C}{\partial \gamma_i} \mathbf{u}_i^C = -\frac{p}{\gamma_i} \mathbf{v}_i^{CT} \mathbf{F}_i \tag{3.11}$$

(2) If i^{th} element is inside to the region R, the first term is non-zero.

$$\frac{\partial U_R^C}{\partial \gamma_i} = \frac{1}{2} \mathbf{u}_i^{CT} \frac{\partial \mathbf{k}_i^C}{\partial \gamma_i} \mathbf{u}_i^C - \mathbf{v}_i^{CT} \frac{\partial \mathbf{k}_i^C}{\partial \gamma_i} \mathbf{u}_i^C = \frac{p}{\gamma_i} (U_i - \mathbf{v}_i^{CT} \mathbf{F}_i) \tag{3.12}$$

where p is the penalty power in SIMP model. U_i is the i^{th} element strain energy. $\mathbf{v}_i^{\Psi}$ is the i^{th} element adjoint displacement vector and $\mathbf{F}_i$ is the i^{th} element nodal force vector.

3.3. Numerical Examples

3.3.1. Package Cushioning Design: Regional Strain Energy Formulation

In this section, the static version of the package cushioning design problem same as Section 2.4 is considered but DCM with the regional strain energy formulation which is shown in Eq. (3.2) is applied. A comparison case which is applied the topology optimization with the regional strain energy formulation is also considered. In this example, all configurations are same as example shown in Section 2.4 and the same model is shown as Figure 2.7.

Three cases are considered and their results are shown in Figure 3.3. Case 1 employs the topology optimization using regional strain energy formulation, i.e. the size of design domain is fixed as initial configuration. Case 2 is the DCM using regional strain energy formulation with large lower bounds. Case 3 is the DCM using regional strain energy with small lower bounds. All cases apply the regional strain energy formulation proposed in this chapter and symmetric boundary conditions. The lower bounds and upper bounds of the cushioning thicknesses, the optimal cushioning thicknesses, the optimal total strain energy, and the optimal strain energy in content are listed in Table 3.1.

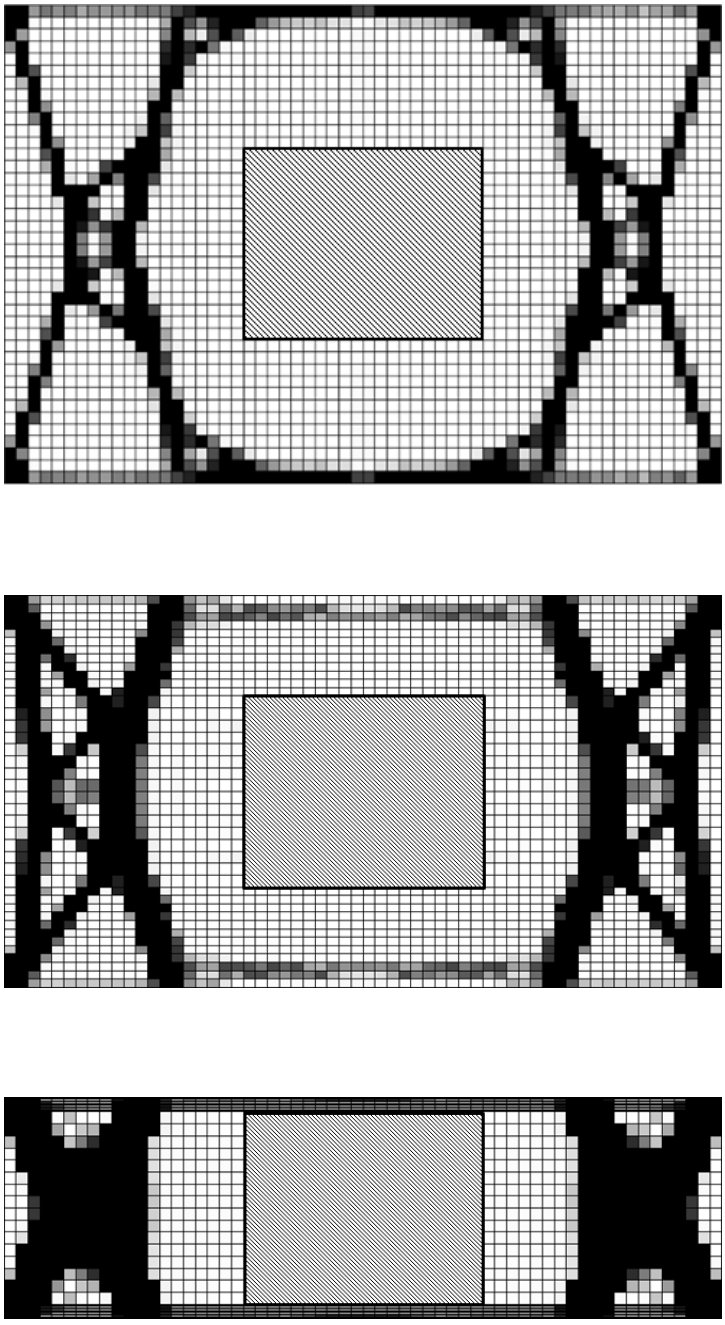

Figure 3.3. Cushioning Design Cases: Case 1. Topology Optimization using Regional Strain Energy Formulation (Top), Case 2. DCM using Regional Strain Energy Formulation with Small Lower Bounds (Middle), Case 3. DCM using Regional Strain Energy Formulation with Large Lower Bounds (Bottom)

Table 3.1. Comparison of Three Results for Package Cushioning Design

Cases	Bounds of Cushioning Dimensions	Dimension of Cushioning	Total Strain Energy	Strain Energy in Content
Case 1: Topology Optimization	a, b, c, d are fixed	$a = 0.2$ $b = 0.2$ $c = 0.12$ $d = 0.12$	436988.7588	0.00157
Case 2: DCM with Large Lower Bounds	$a, b \in [0.14, 0.2]$ $c, d \in [0.084, 0.12]$	$a^* = 0.2$ $b^* = 0.2$ $c^* = 0.084$ $d^* = 0.084$	164345.8086	0.00001
Case 3: DCM with Small Lower Bounds	$a, b \in [0.02, 0.2]$ $c, d \in [0.012, 0.12]$	$a^* = 0.2$ $b^* = 0.2$ $c^* = 0.012$ $d^* = 0.012$	44322.8410	0.000001

In Table 3.1, the dimensions of cushioning are different in difference cases. In Case 1, length and height of the design domain are fixed. In Case 2 and Case 3, length and height of the design domains are bounded and the lower bounds are different: one is large and another one is small. The results of these two cases converge to the given bounds: lengths reach their upper bounds and heights reach their lower bounds. The objective functions of all cases are multiplication of total strain energy of the whole structure and regional strain energy of the content. The total strain energy values and the regional strain energy values are decrease from Case 1 to Case 3.

To present the structural deformations, strain energy distributions of the optimal designs are shown in Figure 3.4 and all cases are plotted in the same contour legend

range. Case 2 and 3 present smaller strain energy distributions than Case 1 and it is consistent with the strain energy results in Table 3.1.

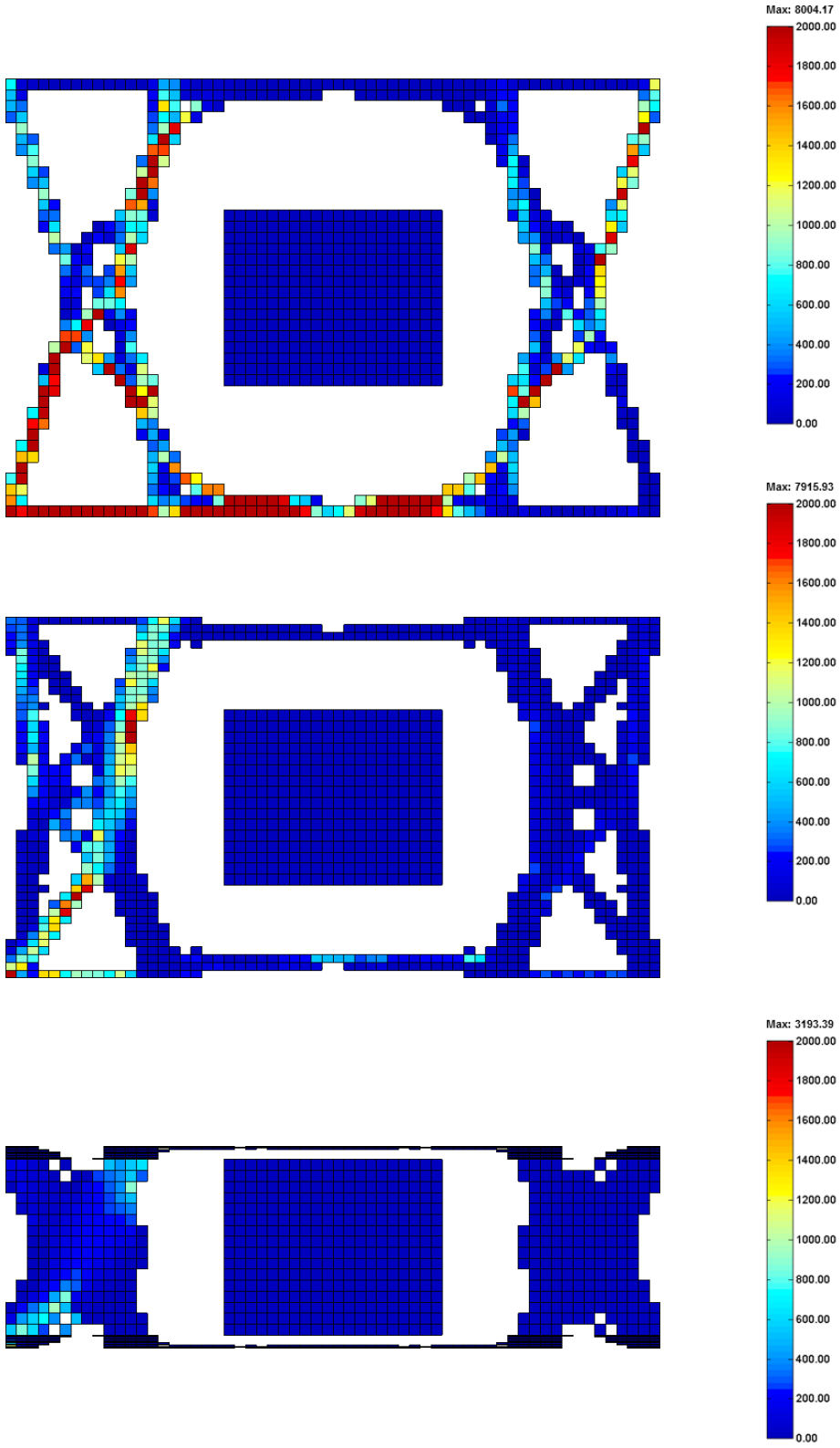

Figure 3.4. Strain Energy Distributions of Cushioning: Case 1. Topology Optimization using Regional Strain Energy Formulation (Top), Case 2. DCM using Regional Strain Energy Formulation with Small Lower Bounds (Middle), Case 3. DCM using Regional Strain Energy Formulation with Large Lower Bounds (Bottom)

This example shows the effectiveness of DCM using regional strain energy formulation. All cases are given structures which bypass the protected content so the regional strain energies of contents are very small, actually almost zeros. They are reasonable results because no force directly acts on the content. The optimal objective function values, i.e. the multiplication of the regional strain energy of content and the total strain energy of the entire structure, are reduced in Case 2 and Case 3 comparing with Case 1, so DCM gives a better solution than topology optimization method.

3.3.2. Support Structure: Table Design

The second example of this chapter is a table design which is applied DCM using regional strain energy formulation proposed as Eq. (3.2). There are two purposes to present this example: (1) this is an extended application of DCM using the regional strain energy formulation; (2) this example demonstrates that designable domain and non-designable domain for material distribution still can tradeoff materials because of subdomain size changes.

As shown in Figure 3.5, the design domain, boundary condition and external load are symmetric so only half of table is considered and the symmetric boundary condition is applied which left edge of half table is supported horizontally.

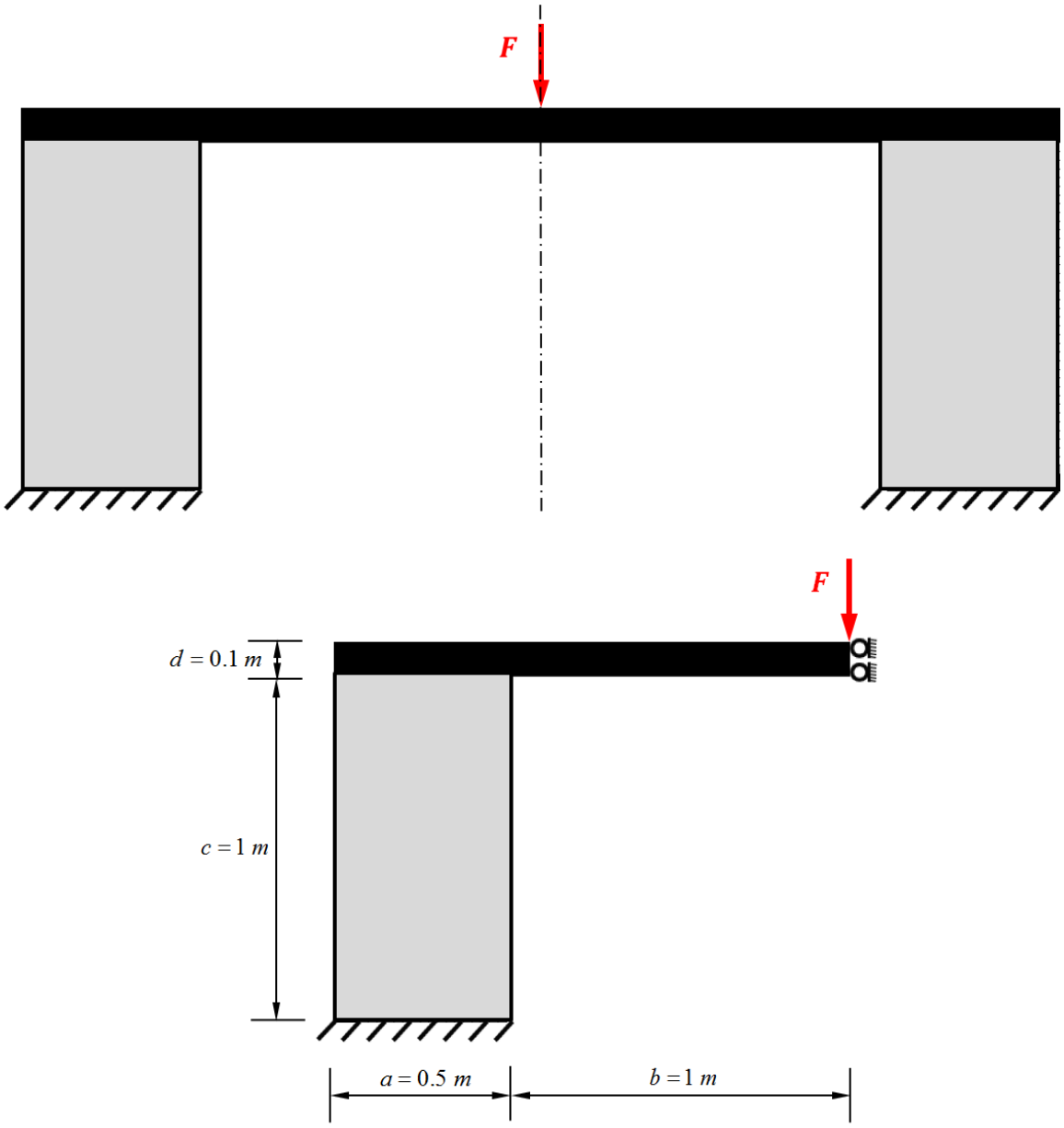

Figure 3.5. Symmetric Boundary Condition and Initial Design Domain for Table Design

The initial dimensions of the half table are given in Figure 3.5. The bottom edge is fixed and the external load $F = 1000kN$ is applied at the center table top. The design requirements and geometric constraints are listed as follows: (1) minimize the deformation of the table top and minimize the deformation of the whole table at the same

time; (2) the total weight of the table is fixed, i.e. the total material including table top and supports is fixed; (3) the thickness of table top is changeable but the total height of the table is fixed: $d \in [0.075, 0.125]$ and $c + d = 1.1$; (4) the under table space is fixed, i.e. $b = 1$ is fixed; (5) the supports design area dimensions is changeable. The lower bounds and upper bounds of dimensions are: $a \in [0.25, 0.5]$, $b = 1$ and it is fixed, $c \in [0.975, 1.025]$, $d \in [0.075, 0.125]$. The material properties are set as follows: Young's modulus $E_0 = 20GPa$, Poisson's ratio $\nu = 0.3$. The volume constraint is applied as: the table top area is fulfilled with material and the table support area is 30% material as the initial. The entire design domain is meshed by four node quadrilateral (Q4) elements.

Two cases are shown in Figure 3.6 and Figure 3.7. The first case is used for comparison purposes: it employs topology optimization using the regional strain energy formulation. The domain is fixed as the initial design. The second case holds DCM using the regional strain energy formulation. In this design, material can be collaborated between table top and supports even the table top has the fixed material distribution. The optimal dimensions of the table, the optimal total strain energy value and the optimal strain energy values in table top are listed in Table 3.2.

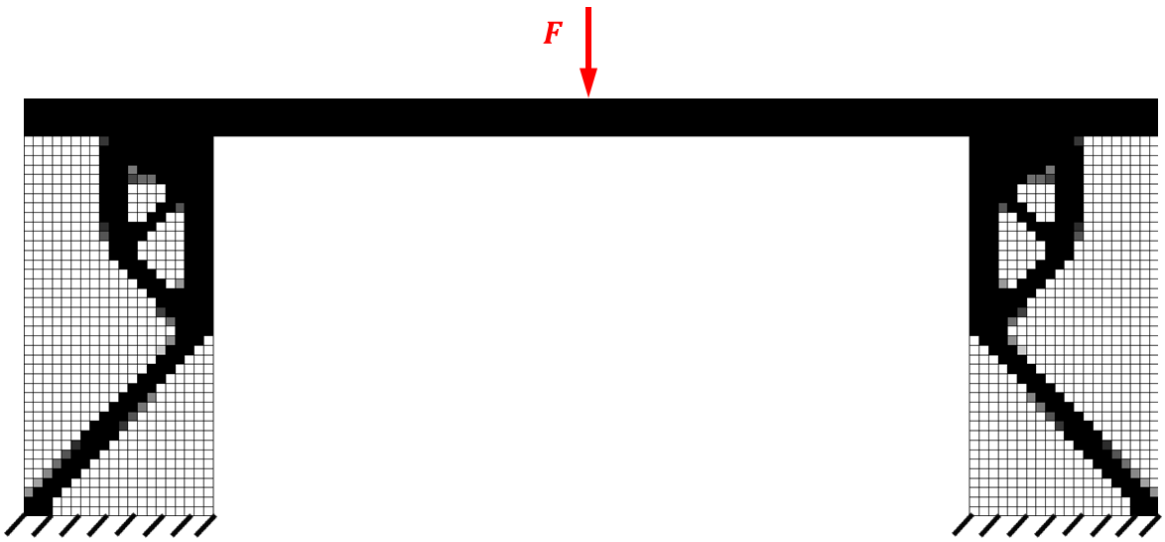

Figure 3.6. Topology Optimization using Total Strain Energy Formulation

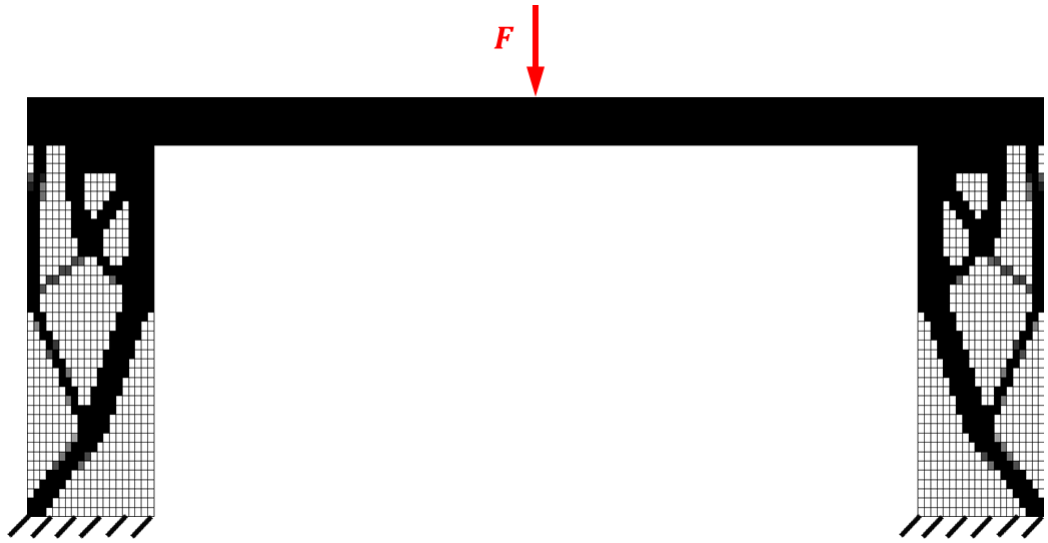

Figure 3.7. DCM using Regional Strain Energy Formulation

Table 3.2. Results Comparison of Table Design

Case	Bounds of Dimensions	Optimal Dimensions	Total Strain Energy the Table	Regional Strain Energy of the Table Top

Case 1: Topology Optimization using Total Strain Energy Formulation	a, b, c, d are fixed	$a = 0.5$ $b^* = 1$ $c^* = 1$ $d^* = 0.1$	297.8566	271.6581
Case 2: DCM using Regional Strain Energy Formulation	$a \in [0.25, 0.5]$ b is fixed $c \in [0.975, 1.025]$ $d \in [0.075, 0.125]$	$a^* = 0.332$ $b^* = 1$ $c^* = 0.975$ $d^* = 0.125$	170.4268	147.3788

In the first design, c converges to the lower bound and d converges to the upper bound. The dimension a is not pushed to its bounds but reaches the optimal value. The total strain energy and regional strain energy in the second design are all smaller than the first design. Thus, DCM using regional strain energy formulation gives a better solution than topology optimization using total strain energy in this table design problem. Also, the material is moved from the table support to the table top because of subdomain size change even the table top is non-designable for material design variables.

3.4. Conclusion

In this chapter, the regional strain energy using DCM for the protective structure is proposed. The protective structure is discussed and the design target of the protective structure is analyzed. The total strain energy is not fit for this design target because the strain energy might be pushed from the protective design domain to the non-designable protected content. A regional strain energy formulation was developed based on the work of Gea [51]. This formulation tries to minimize the deformation in the non-designable content region and generate a structure in the designable region. The sensitivity of two types of design variables are derived and simplified. Two numerical examples are

discussed in this chapter: one is a package cushioning design which is same as Chapter 2 but applies the regional strain energy formulation proposed in this chapter; another one is a table design which extends the application of the proposed regional strain energy formulation.

Chapter 4. Domain Composition Method (DCM) with Inertia Relief Analysis

The new regional strain energy formulation is used in DCM to design protective structures in the previous chapter. The governing equation is static analysis, i.e. the external loads are static loads and the structure response is evaluated under the static situation. This chapter DCM is expanded to consider the dynamic response of the structure. The inertia relief analysis is applied to DCM.

4.1. Protective Structure under Dynamic Load

The typical protective structures are civil structure, bridge infrastructure, ship frame, vehicle frame and packaging. For example, the electrical vehicle while body provides the support and protection for the battery pack when a vehicle crash happened; and the package cushion structure undergoes drop and impact in storage, transportation and delivery. In these two examples, the design targets are protecting the battery pack for electrical vehicle or inside content for the package. The regional strain energy using domain composition method can applied the structure and the location of the battery pack and the content.

A typical package drop example is shown in Figure 4.1. The package of this example consists of three parts: content, cushion and box. The box is made of by the corrugated board but it will not be considered in our research for simplification. The simplified 2D model including content and cushioning is shown in Figure 4.2.

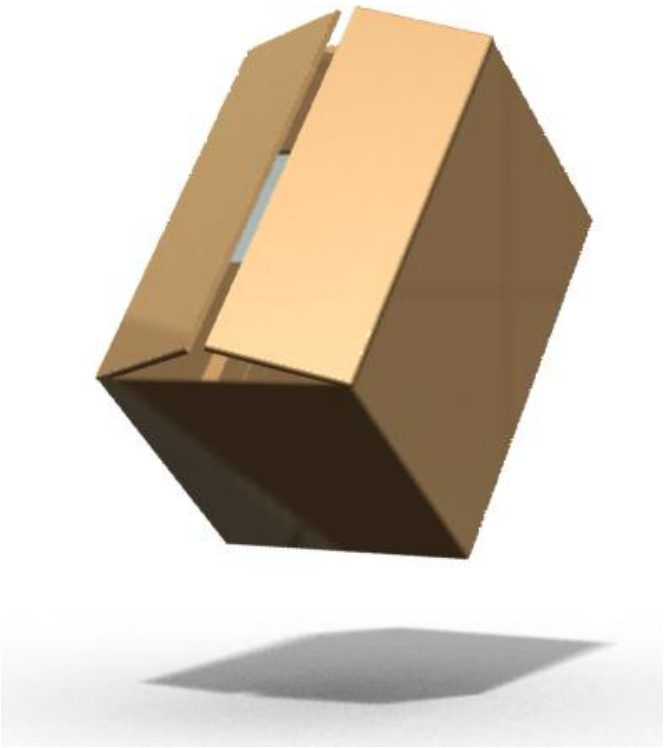

Figure 4.1. A Typical Package Drop Example

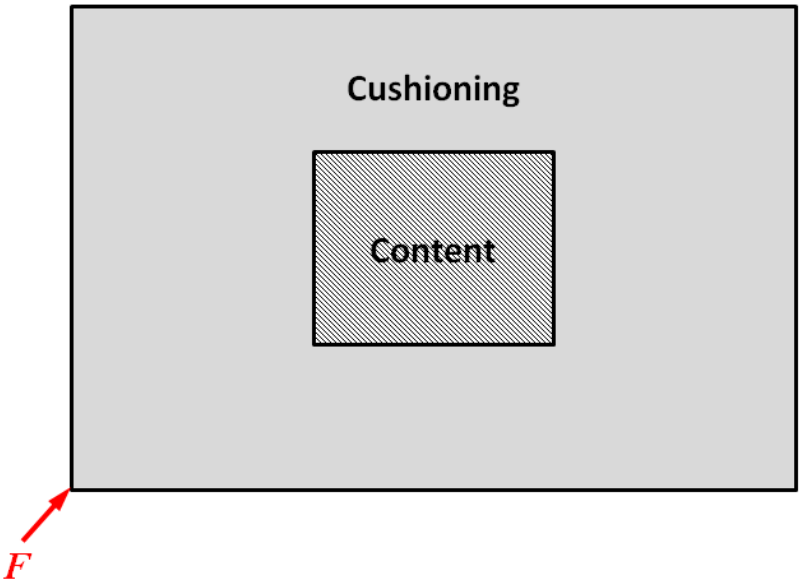

Figure 4.2. Simplified 2D Pacakage Drop without Box

The left bottom corner load **F** is applied to the cushioning. The structure is unbalance because no constraint is applied on the structure in this model. The structure response is dynamically. The transient analysis in finite element theory can be selected to analyze the deformation. However, the computational cost of dynamic analysis is much higher than that of static analysis [58]. The computation of the sensitivity required by a gradient-based optimizer is also complex in dynamic analysis [52]. In order to address these issues, inertia relief analysis can be applied in topology optimization. It takes into account the dynamic effects but utilizes the static analysis, thus saving a substantial amount of computation time and cost [53].

4.2. Inertia Relief Analysis

It is assumed that only steady-state loads act on the system, and the system's transient responses have damped out [67]. The unconstrained structure cannot be performed by static analysis because the stiffness matrix is singular due to rigid body motion of the structure. With the inertia relief technique, an external load is balanced by a set of inertia forces with respect to a reference point. The reference point removes the rigid body motion from the structure, and only elastic deformations are considered. Thus the unconstrained structure is in a state of static equilibrium. A set of inertia forces are calculated through the rigid body acceleration at the reference point and which can be calculated from the rigid body dynamics.

A diverse types of inertia relief techniques have been developed and published by Gaffrey and Lin for Nastran in 1994 [68], Barnett et al. in 1995 [67], Moulin and Karpel in 1998 [69], ANSYS in 2007 [70] and ABAQUS in 2008 [71]. The concise description was drawn by Lee et al. in [72].

The total displacement vector $\mathbf{u}^t$ of the constrained structure can be decomposed into a rigid body displacement vector with respect to the reference point $\mathbf{u}^r$ and an elastic displacement $\mathbf{u}^e$ as

$$\mathbf{u}^t = \mathbf{u}^r + \mathbf{u}^e \tag{4.1}$$

The corresponding total acceleration vector is

$$\ddot{\mathbf{u}}^t = \ddot{\mathbf{u}}^r + \ddot{\mathbf{u}}^e \tag{4.2}$$

When a steady-state external force vector $\mathbf{F}$ is applied to the unconstrained structure with global mass matrix $\mathbf{M}$ and global stiffness matrix $\mathbf{K}$, the dynamic equilibrium equation can be written as

$$\mathbf{K}\mathbf{u}^r + \mathbf{K}\mathbf{u}^e + \mathbf{M}\ddot{\mathbf{u}}^r + \mathbf{M}\ddot{\mathbf{u}}^e = \mathbf{F} \tag{4.3}$$

In this equation, $\mathbf{K}\mathbf{u}^r = \mathbf{0}$ because the rigid body displacement generate zero resultant forces. Also, it is assumed that the inertia force due to the elastic deformation of the structure is negligibly small compared to the one due to the rigid body motion. Thus the relative acceleration term $\mathbf{M}\ddot{\mathbf{u}}^e$ can be omitted from Eq. (4.3)

$$\mathbf{K}\mathbf{u}^e + \mathbf{M}\ddot{\mathbf{u}}^r = \mathbf{F} \tag{4.4}$$

All the applied loads and the inertia forces generated by the applied loads must be balanced at the reference point to achieve force and moment equilibrium. The location of the j^{th} node of the discretized system following the finite element model is described in a Cartesian coordinate system as $\left(x_j, y_j, z_j\right)$. If the coordinate origin is selected as the

reference point at origin $O(0,0,0)$, a geometric rigid body transformation matrix $\mathbf{R}_{oj}$ that relates rigid body motions $\mathbf{u}_o^r$ from the origin to those motions at the j^{th} node $\mathbf{u}_j^r$ can be defined as

$$\mathbf{u}_j^r = \mathbf{R}_{oj}\mathbf{u}_o^r \tag{4.5}$$

where

$$\mathbf{R}_{oj} = \begin{bmatrix} 1 & 0 & -y_j \\ 0 & 1 & x_j \end{bmatrix}.$$

If a reference point is different from the origin, such as the center of gravity (CG), the geometric rigid body transformation matrix is revised accordingly. The choice of the reference point is arbitrary and does not affect the deformation (strain and stress results) of inertia relief although the displacement field is different.

Using the same rigid transformation matrix, the acceleration and force vectors can be transformed as follows

$$\ddot{\mathbf{u}}_j^r = \mathbf{R}_{oj}\ddot{\mathbf{u}}_o^r \tag{4.6}$$

$$\mathbf{R}_{oj}^T\mathbf{F}_j = \mathbf{F}_{oj} \tag{4.7}$$

For a structure discretized by the finite element model with *n* nodes, only a partial of nodal loads applied but others can be treated as zero load vectors applied. The accelerations at the origin and the total resultant load vector can be obtained as

$$\ddot{\mathbf{u}}^r = \mathbf{R}_o\ddot{\mathbf{u}}_o^r \tag{4.8}$$

$$\mathbf{R}_o^T\mathbf{F} = \mathbf{F}_o \tag{4.9}$$

Similar as Eq. (4.9), the inertia force at all nodes can be transformed to the inertia forces at the origin as

$$\mathbf{R}_o^T\mathbf{M}\ddot{\mathbf{u}}^r = \mathbf{R}_o^T\mathbf{M}\mathbf{R}_o\ddot{\mathbf{u}}_o^r \tag{4.10}$$

where $\mathbf{M}$ is the global mass matrix of the structure.

In inertia relief analysis, the total external load applied to the structure at the origin is balanced by the nodal inertia forces about the origin. It can be described as

$$\mathbf{R}_o^T\mathbf{M}\mathbf{R}_o\ddot{\mathbf{u}}_o^r = \mathbf{R}_o^T\mathbf{F} \tag{4.11}$$

Combined with Eq. (4.11), the elastic displacement $\mathbf{u}^e$ can be found through the following equation

$$\mathbf{K}\mathbf{u}^e + \mathbf{M}\mathbf{R}_o\ddot{\mathbf{u}}_o^r = \mathbf{F} \tag{4.12}$$

This is the governing equation for the inertia relief analysis when the origin of the structure is chosen as the reference point for the rigid body motion.

Since the global stiffness matrix $\mathbf{K}$ in Eq. (4.12) is singular for the unconstrained structure, it requires some special techniques to solve for the elastic displacement. A solution method will be explained in this section.

This method is based on the fact that the elastic displacement is orthogonal or decoupled from eigen-solution of an arbitrary rigid body mode shape $\boldsymbol{\varphi}_l$. The geometric rigid body transformation matrix $\mathbf{R}_o$ can be expressed as a linear combination of all rigid body modes. Therefore, the rigid body decoupling condition can be described as follows.

$$\boldsymbol{\varphi}_l^T \mathbf{M}\mathbf{u}^e = 0 \ \text{ for } \forall l \ \rightarrow \ \mathbf{R}_o^T \mathbf{M}\mathbf{u}^e = \mathbf{0} \tag{4.13}$$

Combining Eq. (4.10), (4.12)and(4.13) yields

$$\underbrace{\begin{bmatrix} \mathbf{K} & \mathbf{M}\mathbf{R}_o \\ \mathbf{R}_o^T\mathbf{M} & \mathbf{R}_o^T\mathbf{M}\mathbf{R}_o \end{bmatrix}}_{\text{A nonsigular matrix}} \begin{Bmatrix} \mathbf{u}^e \\ \ddot{\mathbf{u}}_o^r \end{Bmatrix} = \begin{Bmatrix} \mathbf{F} \\ \mathbf{R}_o^T\mathbf{F} \end{Bmatrix} \tag{4.14}$$

Solving Eq. (4.14) gives the rigid body acceleration and elastic displacement simultaneously.

4.3. Domain Composition Method (DCM) with Inertia Relief Analysis

4.3.1. Problem Formulation

To extend the use of the proposed method, DCM involving inertia relief analysis are considered. In the package cushioning design problem shown in Figure 4.2, the outside cushioning regions are designable and the inside content region is non-designable. Because protection of the content is our design target, the regional strain energy formulation is utilized. The content is fixed, but size of the outside design domain is changeable. The difference of this work is that the inertia relief analysis is used in DCM with a regional strain energy formulation.

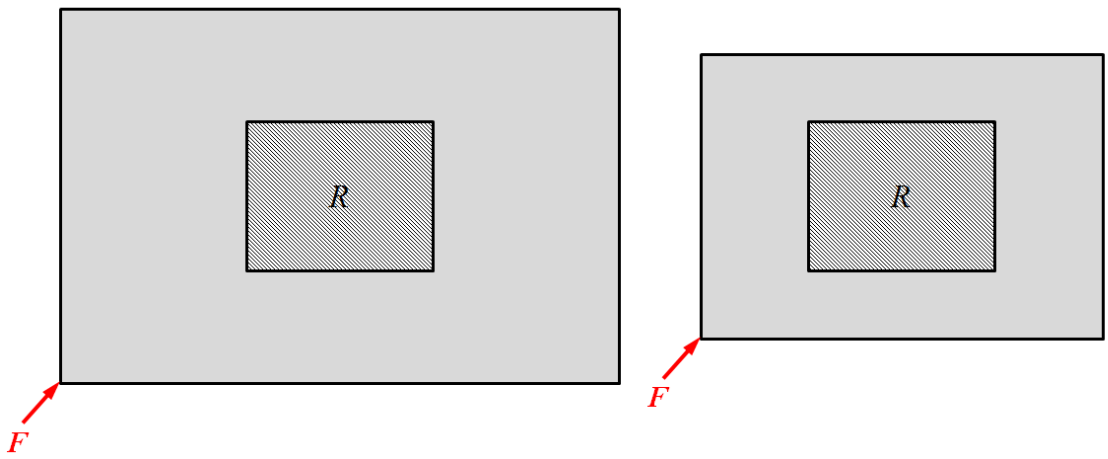

Figure 4.3. Region R in Initial Design I and Current Design C

In the current design C (left in Figure 4.3), a regional strain energy formulation using DCM with inertia relief structural optimization problem is presented as

$$\begin{aligned} &Min:\ U_R^C \cdot U_T^C \\ &s.t.:\ \ \mathbf{K}^C\mathbf{u}^{eC} + \mathbf{M}^C\mathbf{R}_o^C\ddot{\mathbf{u}}_o^{rC} = \mathbf{F} \\ &\qquad V^C(\boldsymbol{\gamma},\boldsymbol{\lambda}) \le \overline{V} \\ &\qquad 0 < \gamma_{\min} \le \gamma_i \le 1,\ \ i = 1,\cdots,N \\ &\qquad 0 < \underline{\lambda}_j \le \lambda_j \le \overline{\lambda}_j,\ \ j = 1,\cdots,M \end{aligned} \tag{4.15}$$

where $\overline{V}$ is the volume bound which is predefined by designer. N is the total element number in design domain. M is the number of scaling factors which are defined in different subdomains.

4.3.2. Inertia Relief Analysis using DCM

The inertia relief analysis governing equation for the current design is

$$\mathbf{K}^C\mathbf{u}^{eC} + \mathbf{M}^C\mathbf{R}_o^C\ddot{\mathbf{u}}_o^{rC} = \mathbf{F} \tag{4.16}$$

In Eq. (4.16), the relation of the global stiffness matrix $\mathbf{K}^C$ between the current design C and the initial design I is the same as Eq. (2.14) in static analysis. The global mass matrix $\mathbf{M}^C$ is assembled from element mass matrix $\mathbf{m}_e^\Psi$. Similar as element stiffness matrix in Section 2.2.3, , the element consistent mass matrix $\mathbf{m}_e^C$ is calculated as follows [73] for Q4 element.

$$\mathbf{m}_e^\Psi = \int_{V_e} \mathbf{N}^T \mathbf{N} \rho dV = \int_{-1}^{1}\int_{-1}^{1} \mathbf{N}^T \mathbf{N} \rho J^\Psi d\xi d\eta \tag{4.17}$$

where ρ is the material density and $\mathbf{N}$ is the shape function matrix which is nothing related to the nodal coordinates

$$\mathbf{N} = \begin{bmatrix} N_1 & 0 & N_2 & 0 & N_3 & 0 & N_4 & 0 \\ 0 & N_1 & 0 & N_2 & 0 & N_3 & 0 & N_4 \end{bmatrix}$$

and

$$N_1 = \frac{1}{4}(1-\xi)(1-\eta),\ N_2 = \frac{1}{4}(1+\xi)(1-\eta),\ N_3 = \frac{1}{4}(1+\xi)(1+\eta),\ N_4 = \frac{1}{4}(1-\xi)(1+\eta).$$

From Eq. (2.9), the element mass matrix equals to

$$\mathbf{m}_e^\Psi = \lambda_x \lambda_y \int_{-1}^{1}\int_{-1}^{1} \mathbf{N}^T \mathbf{N} \rho J^\Omega d\xi d\eta \tag{4.18}$$

Comparing Eq. (4.18) to the element mass matrix for the initial domain Ω

$$\mathbf{m}_e^\Psi = \int_{-1}^{1}\int_{-1}^{1} \mathbf{N}^T \mathbf{N} \rho J^\Omega d\xi d\eta \tag{4.19}$$

It obtains

$$\mathbf{m}_e^{\Psi} = \lambda_x \lambda_y \mathbf{m}_e^{\Omega} \tag{4.20}$$

The geometric rigid body transformation matrix $\mathbf{R}_o^C$ in the current design domain can be built from nodal transformation matrices about the origin as

$$\mathbf{R}_o^C = \begin{bmatrix} \mathbf{R}_{o1}^{\Psi} \\ \mathbf{R}_{o2}^{\Psi} \\ \vdots \\ \mathbf{R}_{oN}^{\Psi} \end{bmatrix} \text{ and } \mathbf{R}_{oj}^{\Psi} = \begin{bmatrix} 1 & 0 & -y_j^{\Psi} \\ 0 & 1 & x_j^{\Psi} \end{bmatrix} \tag{4.21}$$

where $\mathbf{R}_{oj}^{\Psi}$ is the j^{th} nodal transformation matrix about the origin in the current domain C and $j = 1, \cdots, N$. $\left\{ x_j^C \quad y_j^C \right\}^T$ is the j^{th} node coordinate in the current domain C.

4.3.3. Sensitivity Analysis

To derive the sensitivity of the objective function w.r.t. the material distribution variable γ_i in (4.15), the chain rule give the same form as Eq. (3.9)

$$\frac{\partial \left(U_R^C \cdot U_T^C \right)}{\partial \gamma_i} = \frac{\partial U_R^C}{\partial \gamma_i} U_T^C + \frac{\partial U_T^C}{\partial \gamma_i} U_R^C \tag{4.22}$$

The total strain energy sensitivity $\partial U_T^C / \partial \gamma_i$ calculation is same as Eq. (2.22) and only the derivative $\partial U_R^C / \partial \gamma_i$ in Eq. (3.3) needs to be derived. To derive the sensitivity of the regional strain energy U_R^C, the adjoint method is applied. U_R^C can be rewritten as

$$U_R^C = \sum_{q \in R} \frac{1}{2} \mathbf{u}_q^{CT} \mathbf{k}_q^C \mathbf{u}_q^C + \mathbf{v}^{CT} \left(\mathbf{F} - \mathbf{K}^C \mathbf{u}^C - \mathbf{M}^C \mathbf{R}_o^C \ddot{\mathbf{u}}_o^{Cr} \right) \tag{4.23}$$

where a Lagrange multiplier vector $\mathbf{v}^C$ is introduced. The second term is equal to zero so the modified objective function is equivalent as the original one. Taking derivative of the new objective function w.r.t a design variable γ_i

$$\frac{\partial U_R^C}{\partial \gamma_i} = \sum_{q \in R} \frac{1}{2} \mathbf{u}_q^{CT} \frac{\partial \mathbf{k}_q^C}{\partial \gamma_i} \mathbf{u}_q^C + \sum_{q \in R} \mathbf{u}_q^{CT} \mathbf{k}_q^C \frac{\partial \mathbf{u}_q^C}{\partial \gamma_i} + \mathbf{v}^{CT} \left(\frac{\partial \mathbf{F}}{\partial \gamma_i} - \frac{\partial \mathbf{K}^C}{\partial \gamma_i} \mathbf{u}^C - \mathbf{K}^C \frac{\partial \mathbf{u}^C}{\partial \gamma_i} - \frac{\partial \mathbf{M}^C}{\partial \gamma_i} \mathbf{R}_o^C \ddot{\mathbf{u}}_o^{Cr} - \mathbf{M}^C \frac{\partial \mathbf{R}_o^C}{\partial \gamma_i} \ddot{\mathbf{u}}_o^{Cr} - \mathbf{M}^C \mathbf{R}_o^C \frac{\partial \ddot{\mathbf{u}}_o^{Cr}}{\partial \gamma_i} \right) \tag{4.24}$$

For a design independent load, the term $\partial \mathbf{F} / \partial \gamma_i = \mathbf{0}$. Since the reference point is not related to the design variables, the geometric rigid body transformation matrix $\mathbf{R}_o^C$ is independent of the design variables, and $\partial \mathbf{R}_o^C / \partial \gamma_i = \mathbf{0}$. To eliminate the unknown $\partial \mathbf{u}_q^C / \partial \gamma_i$ and $\partial \mathbf{u}^C / \partial \gamma_i$ from the sensitivity expression for the structure, vector $\mathbf{v}^C$ can be calculated based on the following equation

$$\left(\frac{\partial \mathbf{u}^C}{\partial \gamma_i} \right)^T \left(\mathbf{K}^C \mathbf{v}^C - \mathbf{K}_R^C \mathbf{u}_R^C \right) = 0 \tag{4.25}$$

where $\mathbf{K}_R^C$ and $\mathbf{u}_R^C$ reassembles element stiffness matrix and element nodal displacement and only those nodes that belong to domain R will give non-zero values in $\mathbf{K}_R^C$ and $\mathbf{u}_R^C$. The solution is

$$\mathbf{K}^C \mathbf{v}^C = \mathbf{K}_R^C \mathbf{u}_R^C \tag{4.26}$$

From which the adjoint vector $\mathbf{v}^C$ can be calculated. It can be treated as an inertia relief analysis with zero acceleration, as it is balanced by external forces, and with no

constraint. The above equation cannot be solved by the inversion of the stiffness matrix because the stiffness matrix of the structure is singular. The applied force vector is the right hand side term $\mathbf{K}_R^C \mathbf{u}_R^C$ and it can be computed through the original inertia relief analysis.

Using Eq. (4.26), Eq. (4.24) can be simplified as

$$\frac{\partial U_R^C}{\partial \gamma_i} = \frac{1}{2}\mathbf{u}_i^{CT}\frac{\partial \mathbf{k}_i^C}{\partial \gamma_i}\mathbf{u}_i^C - \mathbf{v}^{CT}\frac{\partial \mathbf{K}^C}{\partial \gamma_i}\mathbf{u}^C - \mathbf{v}^{CT}\frac{\partial \mathbf{M}^C}{\partial \gamma_i}\mathbf{R}_o^C\ddot{\mathbf{u}}_o^{Cr} \tag{4.27}$$

where $\partial \mathbf{k}_q^C / \partial \gamma_i$ in the first term is non-zero only when $q = i$ and $q \in R$.

The sensitivity of the regional strain energy can be calculated if SIMP model is applied, where p is the penalty power in SIMP model

(1) If the design variable γ_i is inside of the region R:

$$\frac{\partial U_R^C}{\partial \gamma_i} = \frac{p}{\gamma_i}U_i^C - \frac{p}{\gamma_i}\mathbf{u}_i^{CT}\mathbf{f}_i - \frac{1}{\gamma_i}\left(\mathbf{v}_i^{CT}\mathbf{F}_i - \mathbf{u}_i^{CT}\mathbf{f}_i\right) \tag{4.28}$$

(2) If the design variable γ_i is outside of the region R:

$$\frac{\partial U_R^C}{\partial \gamma_i} = -\frac{p}{\gamma_i}\mathbf{u}_i^{CT}\mathbf{f}_i - \frac{1}{\gamma_i}\left(\mathbf{v}_i^{CT}\mathbf{F}_i - \mathbf{u}_i^{CT}\mathbf{f}_i\right) \tag{4.29}$$

The chain rule is applied to calculate the derivative of the objective function w.r.t. the shape variable λ_j as

$$\frac{\partial\left(U_R^C \cdot U_T^C\right)}{\partial \lambda_j} = \frac{\partial U_R^C}{\partial \lambda_j}U_T^C + \frac{\partial U_T^C}{\partial \lambda_j}U_R^C \tag{4.30}$$

The sensitivity of the total strain energy can be calculated as

$$\frac{\partial U_T^C}{\partial \lambda_j} = -\frac{1}{2}\mathbf{u}^{CT}\frac{\partial \mathbf{K}^C}{\partial \lambda_j}\mathbf{u}^C - \mathbf{u}^{CT}\frac{\partial \mathbf{M}^C}{\partial \lambda_j}\mathbf{R}_o^C\ddot{\mathbf{u}}_o^{rC} - \mathbf{u}^{CT}\mathbf{M}^C\frac{\partial \mathbf{R}_o^C}{\partial \lambda_j}\ddot{\mathbf{u}}_o^{rC} \tag{4.31}$$

The derivation of the regional strain energy sensitivity yields a similar result as Eq. (4.27) but the transformation matrix derivative is non-zero because $\mathbf{R}_o^C$ is related the nodal coordinates. The nodal coordinates are functions of the scaling factor λ_j in the current design C.

$$\frac{\partial U_R^C}{\partial \lambda_j} = \sum_{q\in R}\frac{1}{2}\mathbf{u}_q^{CT}\frac{\partial \mathbf{k}_q^C}{\partial \lambda_j}\mathbf{u}_q^C - \mathbf{v}^{CT}\frac{\partial \mathbf{K}^C}{\partial \lambda_j}\mathbf{u}^C - \mathbf{v}^{CT}\frac{\partial \mathbf{M}^C}{\partial \lambda_j}\mathbf{R}_o^C\ddot{\mathbf{u}}_o^{rC} - \mathbf{v}^{CT}\mathbf{M}^C\frac{\partial \mathbf{R}_o^C}{\partial \lambda_j}\ddot{\mathbf{u}}_o^{rC} \tag{4.32}$$

In Eq. (4.31) and (4.32), partial derivative terms are not easy to evaluate because the scaling factor λ_j is related to elements under the range of λ_j. To simplify the calculation, these global terms can be decomposed into elemental terms. If the arbitrary subdomain Ψ in current design and corresponding subdomain Ω in initial design are considered, only derivatives of elemental terms, $\partial\mathbf{k}_e^\Psi/\partial\lambda_j$, $\partial\mathbf{m}_e^\Psi/\partial\lambda_j$, $\partial\mathbf{R}_{oe}^\Psi/\partial\lambda_j$, $\mathbf{k}_e^\Psi$, $\mathbf{m}_e^\Psi$ and $\mathbf{R}_{oe}^\Psi$ are required for each element *e*.

The sensitivity of the element stiffness matrix $\mathbf{k}_e^\Psi$ can be evaluated as Eq. (2.27)-(2.28). From Eq. (4.20), the sensitivity of the element mass matrix $\mathbf{m}_e^\Psi$ is

1) If $\lambda_j = \lambda_{jx}$ or λ_{jy}, the mass sensitivity between current design and initial design is

$$\frac{\partial \mathbf{m}_e^\Psi}{\partial \lambda_j} = \frac{1}{\lambda_j}\mathbf{m}_e^\Psi \tag{4.33}$$

2) If $\lambda_j \neq \lambda_{jx}, \lambda_{jy}$, i.e. λ_j is not related to element e, so

$$\frac{\partial \mathbf{m}_e^{\Psi}}{\partial \lambda_j} = \mathbf{0} \tag{4.34}$$

From Eq. (4.21), the sensitivity of the rigid body transformation matrix for node *k* is

$$\frac{\partial \mathbf{R}_{ok}^{\Psi}}{\partial \lambda_{jx}} = \begin{bmatrix} 0 & 0 & 0 \\ 0 & 0 & \dfrac{\partial x_k^{\Psi}}{\partial \lambda_{jx}} \end{bmatrix} \text{ and } \frac{\partial \mathbf{R}_{ok}^{\Psi}}{\partial \lambda_{jy}} = \begin{bmatrix} 0 & 0 & -\dfrac{\partial y_k^{\Psi}}{\partial \lambda_{jy}} \\ 0 & 0 & 0 \end{bmatrix} \tag{4.35}$$

The coordinate derivatives, such as $\partial x_k^{\Psi} / \partial \lambda_{jx}$ and $\partial y_k^{\Psi} / \partial \lambda_{jy}$ depend on the relationship between the initial design Ω and current design Ψ, and it can be obtained from the scaling and geometry continuity

$$\frac{\partial x^{\Psi}}{\partial \lambda_{jx}} = \begin{cases} 0 & , x^{\Omega} \text{ in the subdomains left of } i \\ x^{\Omega} - x_i^{\Omega} & , x^{\Omega} \text{ in subdomain } i \\ x_{i+1}^{\Omega} - x_i^{\Omega} & , x^{\Omega} \text{ in the subdomains right of } i \end{cases} \tag{4.36}$$

and

$$\frac{\partial y^{\Psi}}{\partial \lambda_{jy}} = \begin{cases} 0 & , \mathrm{y}^{\Omega} \text{ in the subdomians above } i \\ y^{\Omega} - y_i^{\Omega} & , \mathrm{y}^{\Omega} \text{ in subdomain } i \\ y_{i+1}^{\Omega} - y_i^{\Omega} & , \mathrm{y}^{\Omega} \text{ in the subdoamins below } i \end{cases} \tag{4.37}$$

where (x_i, y_i) and (x_{i+1}, y_{i+1}) are the reference points of the scaling of subdomain *i* and $i+1$. The “left”, “right”, “left” and “below” of subdomains are judged by the location of the references points of subdomains.

4.4. Numerical Example: Package Cushioning Design with Inertia Relief

In this section, the package cushioning design is considered which is discussed in Section 4.1. As shown in Figure 4.4, this problem is to find the optimal cushioning structure under dynamic response for package application which protects the inside content, such as weak or fragile products, and obtains a cushioning structure to resist external loads. This structural optimization problem has two objectives: one is minimizing the deformation of the content and another one is minimizing the compliance of the cushioning. On the other hand, the size of the cushioning domain is adjustable. It is straightforward to apply the regional strain energy formulation with DCM to discover the optimal sizes of cushioning and the optimal topology of the structure.

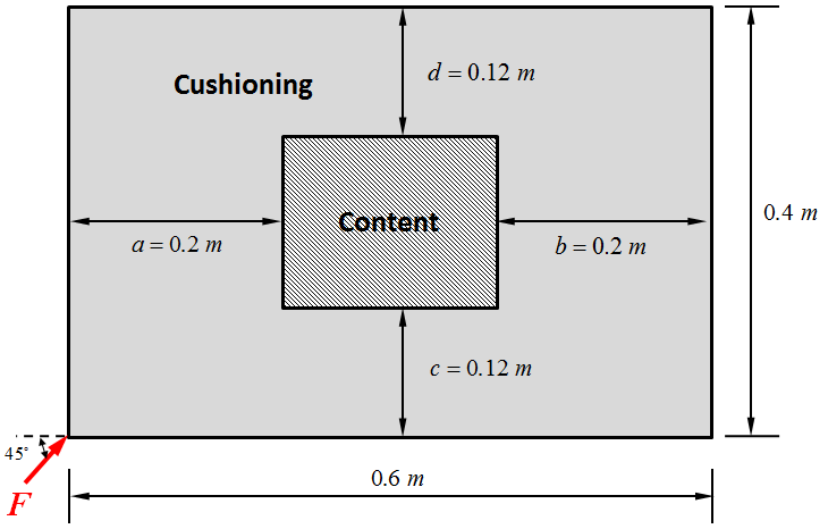

Figure 4.4. Initial Design Domain with no Fixture

The initial configuration of the example is displayed in Figure 4.4 and it is similar as static example in Chapter 2 and 3 except no fixture. The whole system is unconstrained and a nodal force $F = 1414kN$ is acted at the left bottom corner of the design domain. The Inertial Relief (IR) analysis is applied to handle the dynamic response of the structure. The content is at the center of the outside rectangular domain. The design domain is symmetric but the entire domain is considered in our research because initial forces are included in dynamic problem. The initial configuration is modeled as upper bounds of thicknesses of the cushioning and the content size is fixed. The material properties are set as follows. For the content: Young's modulus $E_0 = 20GPa$, Poisson's ratio $\nu = 0.3$ and density $\rho_0 = 2000kg/m^3$; and for the design domain: Young's modulus $E_0 = 0.2GPa$, Poisson's ratio $\nu = 0.3$ and density $\rho_0 = 30kg/m^3$. It shows that the soft cushioning material protects the stiff content. Volume constraint is set as 30% of the total initial cushioning volume and the design domain is meshed by four node quadrilateral (Q4) elements.

Three results are shown in Figure 4.5. All cases are considering as initial relief analysis. Case 1 is the topology optimization using regional strain energy formulation result. Case 2 applies the DCM using the regional strain energy formulation with bounded length and fixed height. Case 3 employs the DCM using the regional strain energy formulation with bounded length and height. The lower bounds and upper bounds of the cushioning thicknesses, the optimal cushioning thicknesses, the total strain energy, and the strain energy in content are listed in Table 4.1.

To present the structural deformations, strain energy distributions of the optimal designs are shown in Figure 4.6 and all cases are plotted in the same contour legend

range. Case 2 and 3 present smaller strain energy distributions than Case 1 and it is consistent with the strain energy results in Table 4.1.

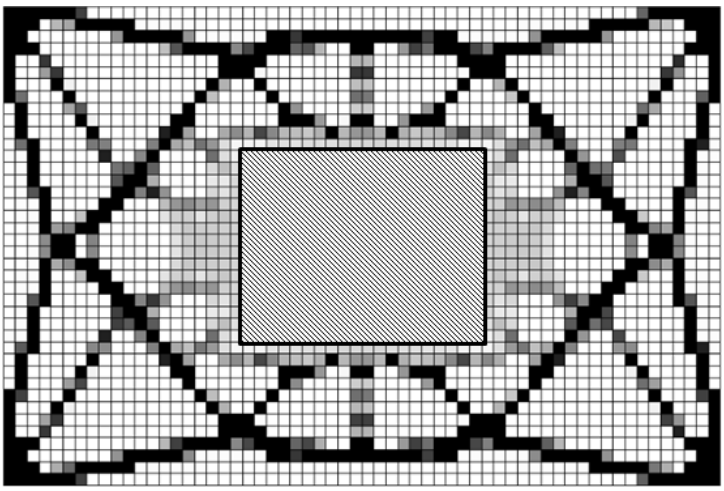

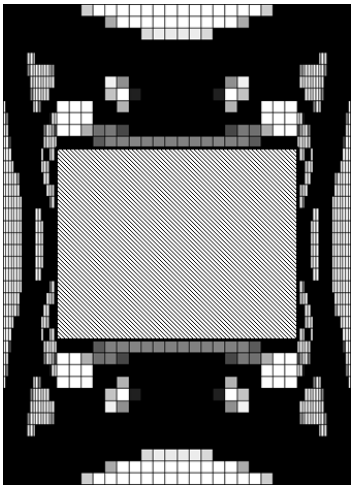

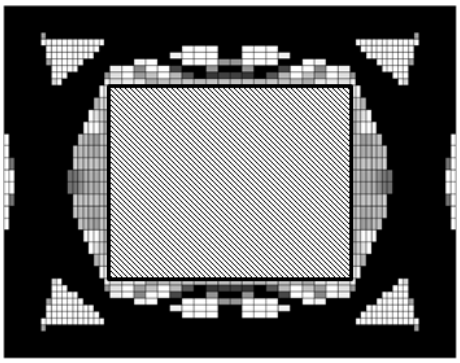

Figure 4.5. Cushioning Design Cases: Case 1. Topology Optimization using Regional Strain Energy with Inertial Relief (Top), Case 2. DCM with Bounded Length and Fixed Height (Middle), Case 3. DCM with Bounded Length and Height (Bottom)

Table 4.1. Comparison of Three Results for Package Cushioning Design

Cases	Bounds of Cushioning	Optimal Dimensions of Cushioning	Total Strain Energy	Strain Energy in Content
Case 1: Topology Optimization using Regional Strain Energy with Inertia Relief	a, b, c, d are fixed	$a = 0.2$ $b = 0.2$ $c = 0.12$ $d = 0.12$	248767.8629	11.5103
Case 2: DCM with Bounded Length and Fixed Height	$a, b \in [0.02, 0.2]$ c, d are fixed	$a^* = 0.045$ $b^* = 0.045$ $c = 0.12$ $d = 0.12$	24312.8352	13.8701
Case 3: DCM with Bounded Length and Height	$a, b \in [0.02, 0.2]$ $c, d \in [0.012, 0.12]$	$a^* = 0.089$ $b^* = 0.089$ $c^* = 0.065$ $d^* = 0.065$	33085.2903	9.9771

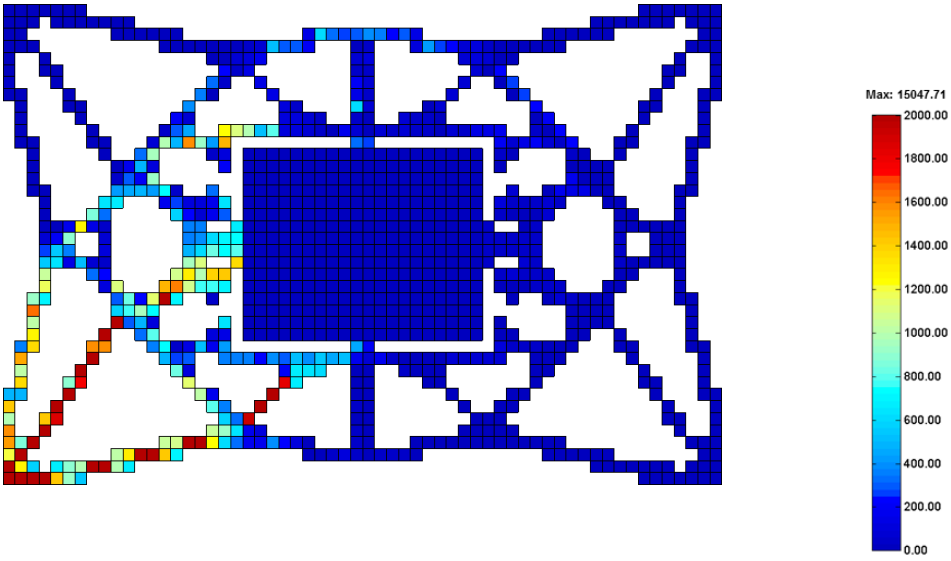
Max: 15047.71
2000.00
1800.00
1600.00
1400.00
1200.00
1000.00
800.00
600.00
400.00
200.00
0.00

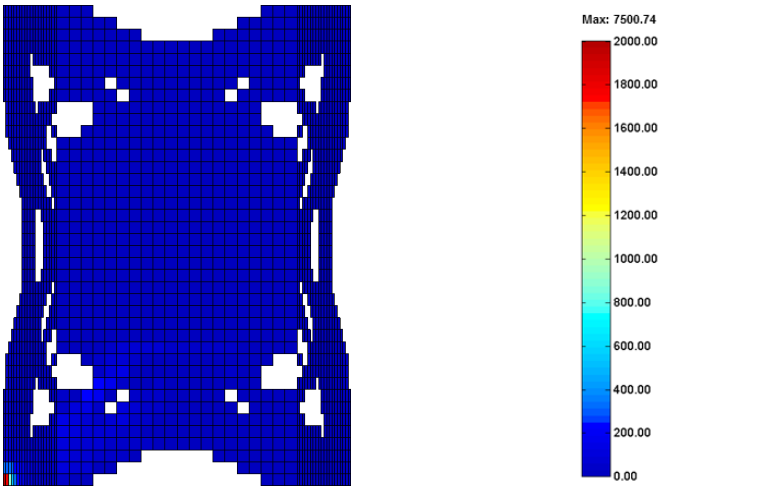
Max: 7500.74
2000.00
1800.00
1600.00
1400.00
1200.00
1000.00
800.00
600.00
400.00
200.00
0.00

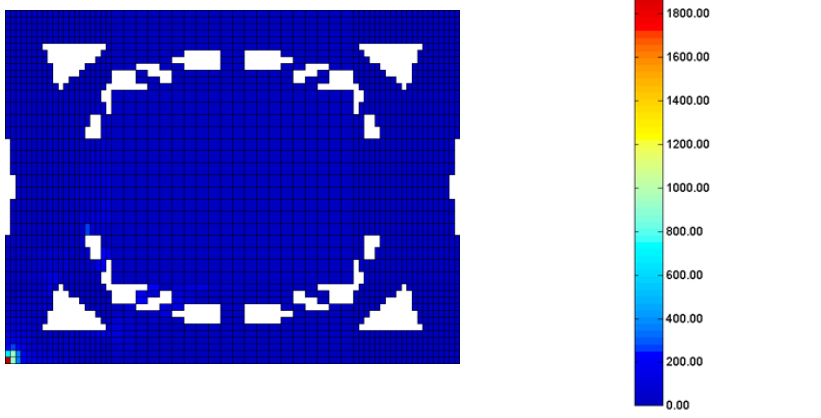
Max: 5231.19
2000.00
1800.00
1600.00
1400.00
1200.00
1000.00
800.00
600.00
400.00
200.00
0.00

Figure 4.6. Strain Energy of Cushioning Design Cases: Case 1. Topology Optimization using Regional Strain Energy with Inertial Relief (Top), Case 2. DCM with Bounded Length and Fixed Height (Middle), Case 3. DCM with Bounded Length and Height (Bottom)

This example shows the effectiveness of DCM using regional strain energy with Inertia Relief (IR). The optimal objective function values, i.e. the multiplication of the total strain energy of the entire structure and the regional strain energy of content, are reduced in Case 2 and Case 3 comparing with Case 1. Therefore, DCM gives better solutions than topology optimization method if the regional strain energy formulation and IR analysis are applied in this cushioning design. Also, it is worth to note all thicknesses converge to the optimal thicknesses instead of bounds in Case 2.

4.5. Conclusion

In practice, the protective structures always undergoes the dynamic loads, such as shock and impact loads for package cushioning in its transportation and delivery, and impact loads for vehicle white body. However, the dynamic transient analysis is much more computational time consuming than the static analysis. So the inertia relief analysis is applied in our research. The equations and solving technique are presented. The structural optimization problem is formulated using DCM with inertia relief. DCM is combined with the inertia relief analysis and the sensitivities for two types of design variables are derived. The cushioning design example is studied to show the effectiveness of our DCM.

Chapter 5. Conclusion and Future Work

Domain Composition Method (DCM) and its extensions to regional strain energy formulation and inertia relief analysis are proposed and the applications in protective structure design are shown in this dissertation. The main conclusions of this research are briefly summarized and further research can be extended based on the research is also discussed in this chapter.

5.1. Conclusion

Conventionally, design domain of topology optimization is fixed. However, if designer has the possibility to change whole or partial of the design domain to obtain a better solution, the tradition topology optimization cannot handle this kind of problem. To fulfill this requirement, DCM is proposed and developed.

DCM provides a way to change the whole or partial of the design domain. It distributes material between elements and subdomains. This method divides design domain into a set of subdomains which sizing change are described by scaling factors. A set of scaling factors is parameterized design domain change between the initial design and the current design that is called subdomain transformation. DCM is applied in static analysis and then integrated into the total strain energy formulation. The proposed optimization problem finds the optimized size and topologies of the structures in those subdomains simultaneously. The sensitivities of the objective function with respect to two kinds of design variables are derived respectively.

DCM using the regional strain energy for the protective structure is also discussed in this dissertation. A typical protective structure, the package cushioning structure, is

discussed and its design target is analyzed. Total strain energy is not proper for this design target because the strain energy might be pushed from the protective design domain to the non-designable protected content. The regional strain energy formulation minimizes the deformation in the non-designable content region and generates a structure in the designable cushioning region. The sensitivities w.r.t. two types of design variables are derived and simplified.

Inertia relief is combined with DCM using regional strain energy formulation. Inertia relief analysis avoids costly transient analysis to find the response of an unconstrained structure subject to constant or slowly varying external loads. The structural optimization problem is formulated as DCM using regional strain energy formulation with inertia relief. DCM is applied to the inertia relief analysis and the sensitivities w.r.t. two types of design variables are derived.

The effectiveness of the proposed methods and formulations are demonstrated in the package cushioning design problems separately from Chapter 2 to Chapter 4. The extended application and two numerical examples are discussed in Chapter 2 and Chapter 3 separately. The cantilever beam with a movable hole beam design is an extended application of the problem defined in Chapter 2. The outside boundary is fixed but the inside boundary is movable. The table design example applies the regional strain energy formulation is discussed in Chapter 3. It shows the regional formulation also can be used in support structure design and it tradeoff material distribution between different subdomains. All numerical examples are verified by comparing DCM results and conventional topology optimization method.

The study in this dissertation about DCM extends the scope of application the structural optimization. It expands the flexibility of the topology optimization to find shape and topology at the same time through design domain change.

5.2. Future Work

This research suggests the concept of DCM and its extension with regional strain energy formulation and inertia relief analysis. However, not all of situations and problems were studied and some possibilities are point out as follows:

- ***More general subdomain transformation***

The study of DCM considers subdomains scaling in this dissertation. However, design change between iterations may be complicate, such as rotation and shear. It can handle more complicate changes of subdomains and DCM becomes more flexible. Correspondingly, more design variables are involved and the next question is how to define these variables automatically. Therefore, more general subdomain transformation might be discussed in the future work.

- ***Automatic mesh update in subdomains in optimization iterations***

In implement of DCM, the finite element meshes are altered corresponding with optimization iterations and it is possible that some elements degenerate distortedly. The distorted elements may increase the magnitude of the error of the finite element solutions. The automatic mesh update might be needed and it depends on the change of elements in design process. This automatic mesh update should be based on some criteria and it may cause material design variables numbers change. Therefore, further study about the automatic mesh update should be conduct.

- ***Other objective function formulation for protective structure design***

In this dissertation, strain energy based objective function is employed. Furthermore, regional strain energy formulation and its sensitivity derivation are presented. However, strain energy is not always a good choice. For example, some cases are requiring minimizing a set of the nodal displacements for some critical points on the structure and average regional displacements may be a better objective function.

- ***Implementation of practical requirements***

In practical situation, some consideration should be combined with DCM discussed in this dissertation to satisfy the practical requirements. For example, structure is always designed bearing multiple load cases and it is a tradeoff results for different situations. Furthermore, the loading conditions are happened with uncertain values and directions, i.e. with load uncertainty. Also, structure always undergoes large displacement and material nonlinearity and nonlinear analysis is required in simulation. Therefore, further study regarding DCM with nonlinearity is worthy.

References

[1] E. Lee, "Stress-Constrained Structural Topology Optimization with Design-Dependent Loads," MR85791 M.A.Sc., University of Toronto (Canada), Toronto, 2012.

[2] J. C. Maxwell, "On Reciprocal Figures, Frames, and Diagrams of Forces," *Earth and Environmental Science Transactions of the Royal Society of Edinburgh,* vol. 26, pp. 1-40, 1870.

[3] M. Lévy, *La statique graphique et ses applications aux constructions: ptie. Principes et applications de statique graphique pure,* 2nd ed. vol. 4. Paris: Gauthier-Villars, 1886.

[4] F. H. Cilley, *The Exact Design of Statically Indeterminate Frameworks, an Exposition of its Possibility, but Futility* vol. 42: Trans. ASCE, 1900.

[5] A. G. M. Michell, "The limits of economy of material in frame-structures," *Philosophical Magazine Series 6,* vol. 8, pp. 589-597, 1904/11/01 1904.

[6] A. M. Brandt, *Criteria and methods of structural optimization* vol. 1: Springer, 1986.

[7] F. R. Shanley, *Weight-strength analysis of aircraft structures*. New York: McGraw-Hill Book Company, 1952.

[8] R. C. Johnson, *Optimum design of mechanical elements*. New York: Wiley, 1961.

[9] V. Venkayya, "Generalized optimality criteria method," *Progress in Astronautics and Aeronautics,* vol. 150, pp. 151-151, 1993.

[10] Z. Wasiutynski, "On the congruency of the forming according to the minimum potential energy with that according to equal strength," *Bull. de l'Academie Polonaise des Sciences, Serie des Sciences Techniques,* vol. 8, pp. 259-268, 1960.

[11] W. Prager and J. Taylor, "Problems of Optimal Structural Design," *Journal of Applied Mechanics,* vol. 35, p. 102, 1968.

[12] J. E. Taylor, "Maximum strength elastic structural design (Elastic sandwich structures design for maximum strength, using potential energy functional to derive governing equations)," *Journal of American Society of Civil Engineers, Engineering Mechanics Division,* vol. 95, pp. 653-663, 1969.

[13] E. F. Masur, "Optimum stiffness and strength of elastic structures," *Journal of the Engineering Mechanics Division,* vol. 96, pp. 621-640, 1970.

[14] M. P. Bendsøe and O. Sigmund, *Topology optimization: theory, methods, and applications*: Springer Verlag, 2003.

[15] L. Chibani, *Optimum design of structures: with special reference to alternative loads using geometric programming*: Springer-Verlag, 1989.

[16] E. J. Haug, K. K. Choi, and V. Komkov, *Design sensitivity analysis of structural systems* vol. 177. New York: Academic Press, 1986.

[17] K. K. Choi and N.-H. Kim, *Structural Sensitivity Analysis and Optimization 1: Linear Systems* vol. 1: Springer, 2005.

[18] K. K. Choi and N.-H. Kim, *Structural Sensitivity Analysis and Optimization 2: Nonlinear Systems and Applications* vol. 2: Springer, 2005.

[19] R. T. Haftka and H. M. Adelman, "Recent developments in structural sensitivity analysis," *Structural optimization,* vol. 1, pp. 137-151, 1989.
[20] O. Zienkiewicz and J. Campbell, "Shape optimization and sequential linear programming," *Optimum structural design,* pp. 109-126, 1973.
[21] S. Bhavikatti and C. Ramakrishnan, "Optimum shape design of rotating disks," *Computers & Structures,* vol. 11, pp. 397-401, 1980.
[22] O. Zienkiewicz, A. Craig, J. Zhu, and R. Gallagher, "Adaptive analysis refinement and shape optimization—some new possibilities," in *The Optimum Shape,* ed: Springer, 1986, pp. 3-27.
[23] Y. Ding, "Shape optimization of structures: a literature survey," *Computers & Structures,* vol. 24, pp. 985-1004, 1986.
[24] R. T. Haftka and R. V. Grandhi, "Structural shape optimization—A survey," *Computer Methods in Applied Mechanics and Engineering,* vol. 57, pp. 91-106, 1986.
[25] Y.-L. Hsu, "A review of structural shape optimization," *Computers in Industry,* vol. 25, pp. 3-13, 1994.
[26] B. Kawohl, A. Cellina, and A. Ornelas, *Optimal Shape Design: Lectures Given at the Joint CIM/CIME Summer School Held in Troia (Portugal), June 1-6, 1998* vol. 1740: Springer, 2000.
[27] B. Zheng, "Topology optimization considering design dependent loadings," Thesis (Ph D), Rutgers University, 2007., 2007.
[28] J. Céa, A. Gioan, and J. Michel, "Quelques résultats sur l'identification de domaines," *Calcolo,* vol. 10, pp. 207-232, 1973.
[29] L. Tartar, "Estimation de coefficients homogenises," in *Computing methods in applied sciences and engineering, 1977, I,* ed: Springer, 1979, pp. 364-373.
[30] M. P. Bendsøe and N. Kikuchi, "Generating optimal topologies in structural design using a homogenization method," *Computer Methods in Applied Mechanics and Engineering,* vol. 71, pp. 197-224, 11// 1988.
[31] H. A. Eschenauer and N. Olhoff, "Topology optimization of continuum structures: A review," *Applied Mechanics Reviews,* vol. 54, p. 331, 2001.
[32] K.-T. Cheng and N. Olhoff, "An investigation concerning optimal design of solid elastic plates," *International Journal of Solids and Structures,* vol. 17, pp. 305-323, 1981.
[33] K. Lurie, A. Cherkaev, and A. Fedorov, "Regularization of optimal design problems for bars and plates, part 1," *Journal of Optimization Theory and Applications,* vol. 37, pp. 499-522, 1982.
[34] R. V. Kohn and G. Strang, "Optimal design and relaxation of variational problems, I," *Communications on Pure and Applied Mathematics,* vol. 39, pp. 113-137, 1986.
[35] R. V. Kohn and G. Strang, "Optimal design and relaxation of variational problems, II," *Communications on Pure and Applied Mathematics,* vol. 39, pp. 139-182, 1986.
[36] R. V. Kohn and G. Strang, "Optimal design and relaxation of variational problems, III," *Communications on Pure and Applied Mathematics,* vol. 39, pp. 353-377, 1986.

[37] K. Suzuki and N. Kikuchi, "A homogenization method for shape and topology optimization," *Computer methods in applied mechanics and engineering,* vol. 93, pp. 291-318, 1991.

[38] J. Thomsen, "Optimization of composite discs," *Structural optimization,* vol. 3, pp. 89-98, 1991.

[39] B. Hassani and E. Hinton, "A review of homogenization and topology optimization I—homogenization theory for media with periodic structure," *Computers & Structures,* vol. 69, pp. 707-717, 12// 1998.

[40] B. Hassani and E. Hinton, "A review of homogenization and topology opimization II—analytical and numerical solution of homogenization equations," *Computers & Structures,* vol. 69, pp. 719-738, 12// 1998.

[41] B. Hassani and E. Hinton, "A review of homogenization and topology optimization III—topology optimization using optimality criteria," *Computers & Structures,* vol. 69, pp. 739-756, 12// 1998.

[42] M. P. Bendsøe, "Optimal shape design as a material distribution problem," *Structural and Multidisciplinary Optimization,* vol. 1, pp. 193-202, 1989.

[43] M. Zhou and G. I. N. Rozvany, "The COC algorithm, Part II: Topological, geometrical and generalized shape optimization," *Computer Methods in Applied Mechanics and Engineering,* vol. 89, pp. 309-336, 8// 1991.

[44] H. P. Mlejnek, "Some aspects of the genesis of structures," *Structural and Multidisciplinary Optimization,* vol. 5, pp. 64-69, 1992.

[45] R. Yang and C. Chuang, "Optimal topology design using linear programming," *Computers & Structures,* vol. 52, pp. 265-275, 1994.

[46] M. P. Bendsøe and O. Sigmund, "Material interpolation schemes in topology optimization," *Archive of Applied Mechanics,* vol. 69, pp. 635-654, 1999.

[47] M. Stolpe and K. Svanberg, "An alternative interpolation scheme for minimum compliance topology optimization," *Structural and Multidisciplinary Optimization,* vol. 22, pp. 116-124, 2001/09/01 2001.

[48] J. Chen, V. Shapiro, K. Suresh, and I. Tsukanov, "Shape optimization with topological changes and parametric control," *International journal for numerical methods in engineering,* vol. 71, pp. 313-346, 2007.

[49] J. Zhu, W. Zhang, P. Beckers, Y. Chen, and Z. Guo, "Simultaneous design of components layout and supporting structures using coupled shape and topology optimization technique," *Structural and Multidisciplinary Optimization,* vol. 36, pp. 29-41, 2008.

[50] J. Zhu, W. Zhang, and P. Beckers, "Integrated layout design of multi-component system," *International Journal for Numerical Methods in Engineering,* vol. 78, pp. 631-651, 2009.

[51] H. Gea, "Applications of regional strain energy in compliant structure design for energy absorption," *Structural and Multidisciplinary Optimization,* vol. 26, pp. 224-228, 2004.

[52] S. Min, N. Kikuchi, Y. C. Park, S. Kim, and S. Chang, "Optimal topology design of structures under dynamic loads," *Structural and Multidisciplinary Optimization,* vol. 17, pp. 208-218, 1999.

[53] H. N. Agrawal, S. G. Kelkar, N. J. Pritula, and R. A. Shipman, "Static analysis using the inertia relief technique to evaluate a hood structure for slam/drop loads," presented at the MSC/Natran User's Conference, 1988.

[54] J. Mahishi, "Nonlinear static and multi-axial fatigue analysis of automotive lower control arm using NEINASTRAN," ed, 2005.

[55] D. W. Sleight and D. M. Muheim, "Parametric studies of square solar sails using finite element analysis," *AIAA*, vol. 1709, p. 45, 2004.

[56] N. Bessert and O. Frederich, "Nonlinear airship aeroelasticity," *Journal of fluids and structures*, vol. 21, pp. 731-742, 2005.

[57] L. Liao and I. Pasternak, "Finite Element Analysis in Novel Aerostructure Design," ed: American Institute of Aeronautics and Astronautics, 1801 Alexander Bell Dr., Suite 500 Reston VA 20191-4344 USA, 2009.

[58] M. Anvari and B. Beigi, "Automotive Body Fatigue Analysis–Inertia Relief or Transient Dynamics?," *SAE Technical Paper*, pp. 01-3149, 1999.

[59] L. Liao, "A Study of Inertia Relief Analysis," presented at the 52nd AIAA/ASME/ASCE/AHS/ASC Structures, Structural Dynamics and Materials Conference, 2011.

[60] N. Pagaldipti and Y. K. Shyy, "Influence of inertia relief on optimal designs," 2004.

[61] G. C. Quinn, "Full Automobile Topology Design Optimized to Maximize Structural Stiffness Subject to Multiple Static Load Cases Including Inertial Relief," *13th AIAA/ISSMO Multidisciplinary Analysis Optimization Conference*, September 13-15, 2010 2010.

[62] X. Huang and Y. Xie, "Evolutionary topology optimization of continuum structures including design-dependent self-weight loads," *Finite Elements in Analysis and Design*, 2011.

[63] A. Rietz, "Sufficiency of a finite exponent in SIMP (power law) methods," *Structural and Multidisciplinary Optimization*, vol. 21, pp. 159-163, 2001/04/01 2001.

[64] S. Liu, G. Cheng, Y. Gu, and X. Zheng, "Mapping method for sensitivity analysis of composite material property," *Structural and multidisciplinary optimization*, vol. 24, pp. 212-217, 2002.

[65] R. D. Cook, D. S. Malkus, and M. E. Plesha, "Concepts and applications of finite element analysis," 1989.

[66] R. T. Marler and J. S. Arora, "Survey of multi-objective optimization methods for engineering," *Structural and multidisciplinary optimization*, vol. 26, pp. 369-395, 2004.

[67] A. R. Barnett, T. W. Widrick, and D. R. Ludwiczak, "Closed-form static analysis with inertia relief and displacement-dependent loads using a MSC/NASTRAN DMAP Alter," *NASA STI/Recon Technical Report N*, vol. 95, p. 19649, 1995.

[68] J. Caffrey and J. M. Lee, *MSC/NASTRAN Linear Static Analysis: User's Guide, Version 68*: MacNeal-Schwendler Corporation, 1994.

[69] B. Moulin and M. Karpel, "Static condensation in modal-based structural optimization," *Structural and Multidisciplinary Optimization*, vol. 15, pp. 275-283, 1998.

[70] ANSYS, "Theory Reference for ANSYS and ANSYS Workbench: Analysis Tool," *Ansys Inc., Version 11.0*, 2007.
[71] I. Abaqus, "ABAQUS Analysis: User's Manual," ed: Vol, 2007.
[72] Y. L. Lee, M. E. Barkey, and H. T. Kang, *Metal fatigue analysis handbook: practical problem-solving techniques for computer-aided engineering*: Butterworth-Heinemann, 2011.
[73] R. D. Cook, *Concepts and applications of finite element analysis*: Wiley. com, 2007.